SIAM J. NUMER. ANAL.
Vol. 57, No. 4, pp. 1545–1573

A HIGHER DEGREE IMMERSED FINITE ELEMENT METHOD BASED ON A CAUCHY EXTENSION FOR ELLIPTIC INTERFACE PROBLEMS*

RUCHI GUO† AND TAO LIN†

Abstract. This article develops and analyzes a pth degree immersed finite element (IFE) method for solving the elliptic interface problems with meshes independent of the coefficient discontinuity in the involved partial differential equations. The proposed pth degree IFE functions are macro polynomials constructed by weakly solving a Cauchy problem locally on each interface element according to the interface jump conditions. To alleviate the discontinuous effects of IFE functions, penalties on both the edges of interface elements and the interface itself are employed in the proposed IFE scheme. New techniques are introduced to analyze the proposed IFE functions in a format of macro polynomials, including their existence, the optimal approximation capabilities of the resulting IFE spaces, and trace inequalities. These results are then further applied to prove that the proposed IFE method converges optimally in both the L^2 and H^1 norms.

Key words. immersed finite element, higher degree macro finite elements, interface independent mesh, elliptic interface problems

AMS subject classifications. 35R05, 65N30, 97N50

DOI. 10.1137/18M121318X

1. Introduction.

In this article, we develop and analyze a pth degree immersed finite element (IFE) method for the second order elliptic interface problem:

$$-\nabla \cdot (\beta \nabla u) = f \quad \text{in } \Omega^- \cup \Omega^+, \tag{1.1a}$$

$$u = 0 \quad \text{on } \partial\Omega, \tag{1.1b}$$

where Ω^- and Ω^+ are the subdomains of $\Omega \subseteq \mathbb{R}^2$ partitioned by a C^{p+1} simple curve Γ which does not intersect $\partial\Omega$. As usual, the following jump conditions are imposed on the interface curve Γ:

$$\mathcal{J}_0(u) = [u]_\Gamma := u^-|_\Gamma - u^+|_\Gamma = 0, \tag{1.1c}$$

$$\mathcal{J}_1(u) = \big[\beta \nabla u \cdot \mathbf{n}\big]_\Gamma := \beta^- \nabla u^- \cdot \mathbf{n}|_\Gamma - \beta^+ \nabla u^+ \cdot \mathbf{n}|_\Gamma = 0, \tag{1.1d}$$

in which $\mathbf{n}$ is the unit normal vector to the interface Γ. Here, β is assumed to be piecewise constants,

$$\beta(X) = \begin{cases} \beta^- & \text{for } X \in \Omega^-, \\ \beta^+ & \text{for } X \in \Omega^+, \end{cases}$$

and, without loss of generality, we assume $\beta^- \geqslant \beta^+$ in the following discussion. In the case $p \geqslant 2$, as in [3, 5, 4], we further impose the so-called Laplacian extended jump conditions

$$\mathcal{J}_j(u) = \left[\beta \frac{\partial^{j-2} \triangle u}{\partial \mathbf{n}^{j-2}}\right]_\Gamma = 0, \quad j = 2, \dots, p. \tag{1.1e}$$

*Received by the editors September 12, 2018; accepted for publication (in revised form) April 10, 2019; published electronically July 3, 2019.
https://doi.org/10.1137/18M121318X
†Department of Mathematics, Virginia Tech, Blacksburg, VA 24061-0123 (ruchi91@vt.edu, tlin@vt.edu).

All the jump conditions in (1.1c)–(1.1e) are imposed in the L^2 sense. The jump conditions in (1.1e) are suggested by the smoothness of the body force term f across the interface curve which is in fact satisfied in many applications such as the constant gravity [48], charge density in electrostatics [32], and the source term in Helmholtz equations [35].

Interface-fitting meshes need to be used in order to obtain the optimal convergence [8, 12, 15, 53] when conventional finite element methods are utilized to solve the interface problem (1.1). In particular, a detailed analysis was given in [38] to show how well the interface must be resolved by the mesh to guarantee the optimal order accuracy according to the degree of polynomials used. By contrast, methods using a fixed mesh for solving the interface problem (1.1) have been developed which, among many benefits, can avoid the time-consuming procedure for generating meshes to fit the interface, especially for those with complicated geometry or evolving shape/location. Roughly speaking, most fixed-mesh methods fall into one of the two groups. A method in the first group fits the interface and the jump conditions by the computation scheme such as the immersed interface method (IIM) [37, 40] in the finite difference context and the CutFEM [14, 28] based on the finite element scheme. In particular, we refer readers to [36, 44, 51] and references therein for higher-order CutFEMs. Methods in the other group take into account the jump behaviors of exact solutions in the construction of shape functions on interface elements such as the multiscale finite element method [16, 19], the extended finite element method [18, 49], the partition of unity method [46, 50], and the immersed finite element (IFE) method to be discussed in this article.

As indicated by the regularity analysis in [16], there are many interface problems in practice, such as the pressure equations from the projection methods solving Naiver–Stokes equations in multifluid dynamics [47] and transmission problems in wave propagation [45], where the exact solutions have a piecewise regularity sufficient for efficiently applying higher degree finite element methods. In addition to the desired high order accuracy, there are also other attractive properties for high order methods, such as their capability to reproduce the oscillatory behavior in high frequency wave propagation problems and their deployment in hp-refinement techniques [6] for efficiently solving problems with localized singularities. These are just a few considerations that motivate us to develop a pth degree IFE method.

One key idea in IFE methods is to use Hsieh–Clough–Tocher [11, 17] type macro elements, i.e., the piecewise polynomials constructed according to the jump conditions, as the shape functions on interface elements while the standard polynomials are used on noninterface elements. Compared with IFE methods based on lower degree polynomials [21, 22, 24, 29, 30, 39, 41, 42] in the literature, there are two major issues in the development of higher degree IFE methods. The first and a fundamental one is to construct suitable macro polynomial spaces on interface elements with the optimal approximation capability to the functions satisfying the jump conditions with respect to the involved polynomial degree. It remains unknown in the literature how to impose suitable weak jump conditions such that the IFE functions universally exist and how to analyze the approximation capabilities of the underlying macro polynomial spaces with discontinuities. The second issue concerns suitable formulation in the related IFE schemes for solving the interface problems. Specifically, this is about suitable penalties to handle the discontinuities of IFE functions on edges and interface. These penalties further pose challenges in the error analysis demanding the trace inequalities for IFE functions as macro polynomials on interface elements because standard trace inequalities cannot apply directly due to insufficient regularity.

There have been exploratory works for higher degree IFE methods. The authors in [2] introduced a correction function to construct the IFE shape functions for the linear interface, and this idea was then generalized in [25] to handle the curved interface for constant coefficient β. The authors in [3] considered an L^2 inner product defined on the actual interface curve to penalize the jump conditions, but the existence of the IFE shape functions based on this approach is not established yet. Recently, the authors in [4, 54] developed a least squares method to construct the IFE shape functions, the existence of which naturally follows from the least squares formulation.

We now propose a construction procedure for pth degree IFE functions. In this procedure, an IFE function is the extension of a pth degree polynomial from one subelement to the whole interface element by solving a local Cauchy problem on interface elements in which the jump conditions across the interface are employed as the boundary conditions. The underlying idea can be traced back to the early works of Babuška, Caloz, and Osborn [7, 9], who proposed special shape functions constructed by solving some local differential equations. This idea was further employed by Chu, Graham, and Hou in [16], where the special shape functions were the piecewise linear finite element solutions of a local interface problem on a submesh of each interface element. We also note that the extension idea from one piece to another in the construction procedure is similar to the one used in [26]. As for the suitable formulation for the related pth degree IFE methods, we propose using penalties on interface edges, like those used in the partially penalized IFE method in [43], and on the interface itself, like those used in CutFEM [44, 51].

The contributions of this article are original and multifold, and we believe they are noteworthy because they enable us to achieve what the conventional construction/analysis techniques in the literature for macro polynomials cannot offer. The core idea, i.e., constructing IFE functions by solving a Cauchy problem locally on each interface element, is originally proposed in this article, and it leads to a so-called Cauchy mapping to connect polynomial components in an IFE function. This mapping also plays a critical role in the related analysis such that major results including the existence of IFE functions, the approximation capabilities, and trace inequalities for the macro polynomials in the proposed IFE space can be traced back to properties of this mapping. The new analysis techniques employed in this article enable us to derive error bounds in which the proportional constants are all independent of the interface location relative to the mesh. All of these together form a systematic framework for us to establish the optimal convergence of the related IFE method as indicated by the following estimate in an energy norm:

$$|\!|\!| u - u_h |\!|\!|_h \lesssim \frac{\beta^+ + \beta^-}{(\beta^+)^{3/2}} h^p \|f\|_{H^{p-1}(\Omega)}.$$

This article consists of five additional sections. In the next section, we introduce basic notations and assumptions. In section 3, we establish a group of geometric estimations and norm equivalence results. In section 4, we introduce a *Cauchy extension* operator and study its properties. In section 5, we use the *Cauchy extension* to define the local IFE spaces, prove the related approximation capability, and trace inequalities. In section 6, we introduce a pth degree IFE method and present an a priori error estimation for this IFE method. Some numerical examples are also presented to demonstrate the convergence of the proposed IFE method.

2. Notations and assumptions. In this section, we introduce some basic notations and assumptions. Given each measurable subset $\widetilde{\Omega} \subseteq \Omega$, we let $W^{k,q}(\widetilde{\Omega})$ be the standard Sobolev space with the norm $\|\cdot\|_{W^{k,q}(\widetilde{\Omega})}$, $k \geqslant 1$, $1 \leqslant q \leqslant \infty$. In the case when $\widetilde{\Omega}$ has a nonempty intersection with the interface Γ, we define $\widetilde{\Omega}^{\pm} = \widetilde{\Omega} \cap \Omega^{\pm}$ and further introduce the following the split space with the associated norm according to the jump conditions (1.1c)–(1.1e):

(2.1a)
$$PW^{k,q}(\widetilde{\Omega}) = \left\{ v \in W^{1,q}(\widetilde{\Omega}) \,:\, v|_{\widetilde{\Omega}^{\pm}} \in W^{k,q}(\widetilde{\Omega}^{\pm});\ \mathcal{J}_i(u) = 0, i = 0, 1, \dots, k-1 \right\},$$

(2.1b)
$$\|v\|_{PW^{k,q}(\widetilde{\Omega})} = \|v\|_{W^{k,q}(\widetilde{\Omega}^{-})} + \|v\|_{W^{k,q}(\widetilde{\Omega}^{+})}.$$

In particular, when $q = 2$, we have the Hilbert spaces $H^k(\widetilde{\Omega})$ and $PH^k(\widetilde{\Omega})$ with the norms $\|\cdot\|_{H^k(\widetilde{\Omega})}$ and $\|\cdot\|_{PH^k(\widetilde{\Omega})}$. Let $PW_0^{k,q}(\widetilde{\Omega})$ and $W_0^{k,q}(\widetilde{\Omega})$ be the related spaces with zero trace on $\partial\widetilde{\Omega}$. We will use $\mathbb{P}_p$ to denote the polynomial space of degree not exceeding p.

We use $\mathcal{T}_h$ to denote a triangular mesh of Ω and let $h = \max_{T \in \mathcal{T}_h}\{h_T\}$, where h_T is the diameter of each element $T \in \mathcal{T}_h$. As usual, we assume the mesh $\mathcal{T}_h$ is shape-regular, i.e., there exists a constant σ such that

$$\frac{h_T}{\rho_T} \leqslant \sigma \quad \forall T \in \mathcal{T}_h, \tag{2.2}$$

where ρ_T is the diameter of the largest inscribed circle of T. It is well known that the condition (2.2) yields the existence of constants $\theta_m, \theta_M \in (0, \pi)$ such that

$$\theta_m \leqslant \text{every angle of } T \leqslant \theta_M \quad \forall T \in \mathcal{T}_h. \tag{2.3}$$

Let $\mathcal{N}_h$ and $\mathcal{E}_h$ be the sets of nodes and edges of the mesh $\mathcal{T}_h$. Denote the sets of interface and noninterface elements in this mesh by $\mathcal{T}_h^i$ and $\mathcal{T}_h^n$. In addition, we let $\mathcal{E}_h^i$ be the collection of all the edges of elements in $\mathcal{T}_h^i$ and let $\mathcal{E}_h^n = \mathcal{E}_h \backslash \mathcal{E}_h^i$.

Guided by [51], given each domain $K \subseteq \mathbb{R}^2$, we call $K' := \{X \in \mathbb{R}^2 : \exists Y \in K \text{ s.t. } \overrightarrow{OX} = \mu\overrightarrow{OY}\}$ the homothetic image of K with respect to the homothetic center O and the scaling constant μ. Hinted by [54], for each interface element $T \in \mathcal{T}_h^i$, we define its fictitious element T_λ as the homothetic image of T with the homothetic center being the incenter G of T and a scaling factor $\lambda \geqslant 1$ independent of mesh size h, and let $\Gamma_T^\lambda = \Gamma \cap T_\lambda$; see Figure 2.1 for an illustration. In particular, we denote $\Gamma_T = \Gamma_T^1 = \Gamma \cap T$. To facilitate a simple presentation of the main ideas, and without loss of generality, we assume that $T_\lambda \subset \Omega$ for every interface element T.

In addition, we employ $|\cdot|$ to denote the measure of a d-dimensional manifold such as edges for $d = 1$ and elements for $d = 2$. Also, following tradition, we employ the notations $\lesssim$ and $\simeq$ to denote the relation $\cdots \leqslant C \cdots$ and the equivalence, respectively, in which the hidden constants C are independent of the mesh size, the coefficients $\beta^{\pm}$ and the local interface location relative to either T or T_λ $\forall T \in \mathcal{T}_h^i$.

Furthermore, we make two major assumptions for the mesh $\mathcal{T}_h$ as follows:

(A1) The mesh is generated such that the interface can only intersect each interface element $T \in \mathcal{T}_h^i$ and its fictitious element T_λ at two distinct points which locate on two different edges of T and T_λ.

(A2) There exists a fixed integer N such that for each $K \in \mathcal{T}_h$, the number of elements in the set $\{T \in \mathcal{T}_h^i : K \cap T_\lambda \neq \emptyset\}$ is bounded by N.

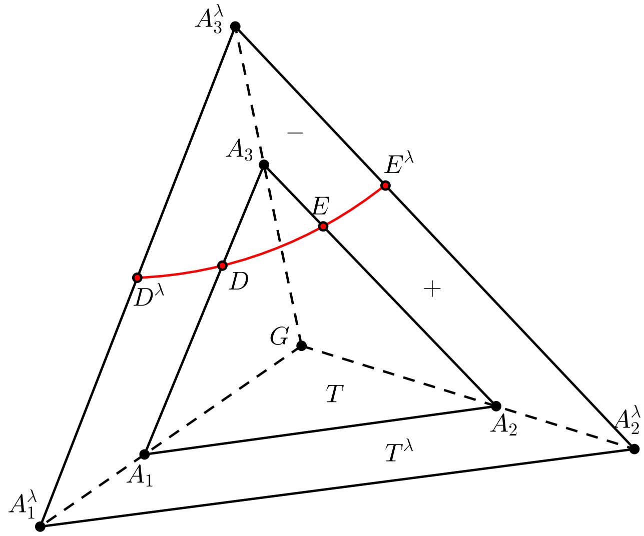

FIG. 2.1. $T = \triangle A_1A_2A_3$ *and its fictitious element* $T_\lambda = \triangle A_1^\lambda A_2^\lambda A_3^\lambda$.

On such a mesh $\mathcal{T}_h$, inspired by [26], we consider the mesh-dependent space V_h as

$$V_h = \{v \in L^2(\Omega) \ : \ v|_T \in H^1(T) \text{ if } T \in \mathcal{T}_h^n, \ v|_{T^\pm} \in H^1(T^\pm) \text{ if } T \in \mathcal{T}_h^i, \\ \text{and } v \text{ is continuous on each } e \in \mathcal{E}_h^n, \ v|_{\partial\Omega} = 0\}, \tag{2.4}$$

and we note that the functions in V_h are in $H^1(\Omega \backslash (\overline{\cup_{T\in\mathcal{T}_h^i} T}))$. Given each $e \in \mathcal{E}_h^i$ shared by two elements T_1 and T_2, we employ the following operators for the functions in V_h:

$$[v]_e = (v|_{T_1})|_e - (v|_{T_2})|_e \quad \text{and} \quad \{v\}_e = \frac{(v|_{T_1})|_e + (v|_{T_2})|_e}{2}, \tag{2.5}$$

and similarly, we can define $[v]_\Gamma$ and $\{v\}_\Gamma$ on the interface. Then, testing (1.1a) by functions in V_h and applying the integration by parts on each element, we obtain the following weak formulation:

(2.6a)

$$a_h(u,v) = L_f(v) \quad \forall v \in V_h,$$

with $a_h(u,v) = \sum_{T\in\mathcal{T}_h} \int_T \beta \nabla u \cdot \nabla v dX$

$$- \sum_{e\in\mathcal{E}_h^i} \int_e \{\beta\nabla u\cdot\mathbf{n}\}_e[v]_e ds + \epsilon_0 \sum_{e\in\mathcal{E}_h^i} \int_e \{\beta\nabla v\cdot\mathbf{n}\}_e[u]_e ds + \sum_{e\in\mathcal{E}_h^i} \frac{\sigma_e^0\gamma}{|e|}\int_e [u]_e\,[v]_e ds \tag{2.6b}$$
$$- \sum_{T\in\mathcal{T}_h^i} \int_{\Gamma_T} \{\beta\nabla u\cdot\mathbf{n}\}_\Gamma[v]_\Gamma ds + \epsilon_1 \sum_{T\in\mathcal{T}_h^i} \int_{\Gamma_T} \{\beta\nabla v\cdot\mathbf{n}\}_\Gamma[u]_\Gamma ds$$
$$+ \sum_{T\in\mathcal{T}_h^i} \frac{\sigma_e^1\gamma}{h_T}\int_{\Gamma_T} [u]_\Gamma\,[v]_\Gamma ds,$$

$$L_f(v) = \int_\Omega f v dX, \tag{2.6c}$$

where σ_e^0 ,σ_e^1 are some constants independent of the coefficients $\beta^\pm$ and $\gamma = (\max\{\beta^-, \beta^+\})^2/\min\{\beta^-, \beta^+\}$. According to (2.6b), we define the following quantities on the space V_h:

$$\|v\|_h^2 = \sum_{T\in\mathcal{T}_h} \int_T \|\sqrt{\beta}\nabla v\|^2 dX + \sum_{e\in\mathcal{E}_h^i} \frac{\sigma_e^0\gamma}{|e|} \int_e [v]_e^2 ds + \sum_{T\in\mathcal{T}_h^i} \frac{\sigma_e^1\gamma}{h_T} \int_{\Gamma_T} [v]_\Gamma^2 ds, \tag{2.7a}$$

$$|||v|||_h^2 = \|v\|_h^2 + \frac{|e|}{\sigma_e^0\gamma} \sum_{e\in\mathcal{E}_h^i} \int_e (\{\beta\nabla v\cdot\mathbf{n}\}_e)^2 ds + \frac{h_T}{\sigma_e^1\gamma} \sum_{T\in\mathcal{T}_h^i} \int_{\Gamma_T} (\{\beta\nabla v\cdot\mathbf{n}\}_\Gamma)^2 ds, \tag{2.7b}$$

and it is easy to verify that these are norms on V_h with

$$\|v\|_h \leqslant |||v|||_h \quad \forall v\in V_h. \tag{2.8}$$

Following the idea in [26], given each $u \in PH_0^{p+1}(\Omega)$, we let $u_E^s \in H_0^{p+1}(\Omega)$ be the Sobolev extensions [20] of $u^s = u|_{\Omega^s}$ from $\Omega^s, s = -, +$ to Ω such that

$$\sum_{k=1}^{p+1} |u_E^s|_{H^k(\Omega)} \leqslant C_E \sum_{k=1}^{p+1} |u^s|_{H^k(\Omega^s)}, \quad s = -, +, \tag{2.9}$$

for some constant C_E only depending on $\Omega^\pm$, Ω, and p. Estimate (2.9) follows from the boundedness for the Sobolev extensions (Theorem 7.25 in [20]) and the Poincaré inequality.

3. Some inequalities on interface elements.

In this section, we first present some basic geometric estimations related to each interface element T and the associated fictitious element T_λ. These results enable us to establish a group of inequalities in the polynomial spaces to be used. Given an interface element $T = \triangle A_1A_2A_3 \in \mathcal{T}_h^i$ with its fictitious element $T_\lambda = A_1^\lambda A_2^\lambda A_3^\lambda$, $\lambda \geqslant 1$, without loss of generality, we only consider the interface element configuration where Γ cuts the edges $A_1^\lambda A_3^\lambda$ and $A_3^\lambda A_2^\lambda$ with the intersection points D^λ and E^λ, as shown by Figure 2.1. We note that the original element and the fictitious element may have different interface configurations; but for simplicity's sake, we also let Γ intersect the original element T with the intersection points D and E at the edges A_1A_3 and A_2A_3. Under this configuration, we let T_λ^- and T_λ^+ be the curved-edge triangle $D^\lambda E^\lambda A_3^\lambda$ and the curved-edge quadrilateral $A_1^\lambda A_2^\lambda E^\lambda D^\lambda$, respectively, as shown in Figure 2.1. Now we start with recalling the following result from [22].

Lemma 3.1. *On each T_λ, $\lambda \geqslant 1$, associated with an interface element $T \in \mathcal{T}_h^i$, assume h_T is small enough; then there exist constants δ_0 and δ_1 independent of the relative interface location inside T_λ and h_T such that for every two points $X_1, X_2 \in \Gamma\cap T_\lambda$ with their normal vectors $\mathbf{n}(X_1), \mathbf{n}(X_2)$ to Γ and every point $X \in \Gamma\cap T_\lambda$ with its orthogonal projection $X^\perp$ onto $D^\lambda E^\lambda$, the following estimations hold:*

$$\|X - X^\perp\| \leqslant \delta_0\lambda^2 h_T^2, \tag{3.1a}$$

$$\mathbf{n}(X_1)\cdot\mathbf{n}(X_2) \geqslant 1 - \delta_1\lambda^2 h_T^2. \tag{3.1b}$$

The estimates (3.1) describe the local flatness of the interface inside each interface element (the special case $\lambda = 1$) and the fictitious element. The constants δ_0, δ_1

depend only on the maximal curvature of Γ [22]. Now we let θ_D and θ_E be the angles between the interface Γ and the ray $D^\lambda A_3^\lambda$, $E^\lambda A_3^\lambda$; see Figure A.1 in the appendix for an illustration. The following lemma describes the relative location of Γ inside T_λ.

LEMMA 3.2. *For each T_λ, $\lambda > 1$, associated with an element $T \in \mathcal{T}_h^i$, assume h_T is small enough; then there exist positive constants θ^λ, l^λ and $r_\lambda^1 \leqslant r_\lambda^2 < 1$ independent of interface location and h_T such that*

$$\angle A_3^\lambda D^\lambda E^\lambda > \theta^\lambda, \quad \angle A_3^\lambda E^\lambda D^\lambda > \theta^\lambda, \quad \theta_D > \theta^\lambda, \quad \theta_E > \theta^\lambda, \tag{3.2a}$$

$$r_\lambda^1 \leqslant \min\left\{ \frac{|A_3^\lambda D^\lambda|}{|A_3^\lambda A_1^\lambda|}, \frac{|A_3^\lambda E^\lambda|}{|A_3^\lambda A_2^\lambda|} \right\} \leqslant r_\lambda^2, \tag{3.2b}$$

$$|\Gamma_T^\lambda| > |D^\lambda E^\lambda| > l^\lambda h_T. \tag{3.2c}$$

Proof. The arguments for these results are technical but elementary; therefore, they are presented in Appendix A.1. ∎

Remark 3.1. Lemma 3.2 actually shows that given each interface element T, the triangular curved-edge subelement of its fictitious element T_λ, $\lambda > 1$, has the regular shape.

Based on the two lemmas above, in the following discussion, we always assume the mesh size h is small enough such that they all hold. Next, we present an estimation of the difference between the Laplacians of the extensions $u_E^\pm$.

LEMMA 3.3. *Let $u \in PH^{p+1}(\Omega)$ with the integer $p \geqslant 1$, and let $u_E^\pm$ be the Sobolev extensions. Then on each fictitious element T_λ, $\lambda > 1$, it holds that*

$$\|\beta^+ \triangle u_E^+ - \beta^- \triangle u_E^-\|_{L^2(T_\lambda)} \lesssim h_T^{p-1}(\beta^+|u_E^+|_{H^{p+1}(T_\lambda)} + \beta^-|u_E^-|_{H^{p+1}(T_\lambda)}). \tag{3.3}$$

Proof. Let $w = \beta^+ \triangle u_E^+ - \beta^- \triangle u_E^- \in H^{p-1}(\Omega)$. Note that the case $p = 1$ is trivial, so we only discuss $p \geqslant 2$. Since $u_E^\pm|_{\Omega^\pm} = u^\pm$, by the definition (2.1a), for $i = 0, 1, \ldots, p-2$, the ith order trace of w on Γ_T^λ is zero.

First, for the curved-edge triangular subelement T_λ^-, according to (3.2a) and Remark 3.1, there exists a one-to-one mapping F [55] from the reference element $\hat{T} = \hat{A}_1\hat{A}_2\hat{A}_3$ with $\hat{A}_1 = (0,0)^T$, $\hat{A}_2 = (1,0)^T$, and $\hat{A}_3 = (0,1)^T$ on the $\hat{x}$-$\hat{y}$ plane to T_λ^- such that its Jacobian satisfies $C_1 h_T^2 \leqslant |\det(\frac{\partial F(\hat{x},\hat{y})}{\partial(\hat{x},\hat{y})})| \leqslant C_2 h_T^2$ for some constants C_1, C_2 independent of the curved edge. Let $\hat{w} = w(F(\hat{x},\hat{y}))$; then the scaling argument together with the Friedrichs inequality for functions vanishing on part of the boundary [1] yields

$$\|w\|_{L^2(T_\lambda^-)}^2 \leqslant Ch_T^2 \|\hat{w}\|_{L^2(\hat{T})}^2 \leqslant Ch_T^2 |\hat{w}|_{H^{p-1}(\hat{T})}^2 \leqslant Ch_T^{2(p-1)} |w|_{H^{p-1}(T_\lambda^-)}^2. \tag{3.4}$$

On the curved-edge quadrilateral T_λ^+, the scaling argument is not applicable directly. Instead, we employ a different approach by constructing a finite number of strips with bounded width to cover the whole quadrilateral T_λ^+ of which the number is bounded independently of the interface inside T_λ. Let P_0 be A_1^λ and P_1 be a point on the edge $A_1^\lambda A_2^\lambda$ such that $A_1^\lambda D^\lambda$ is parallel to $P_1 E^\lambda$, and the first strip s_1 is the curved-edge quadrilateral $A_1^\lambda P_1 E^\lambda D^\lambda$. Then we proceed by induction to find P_n on $A_1^\lambda A_2^\lambda$ such that $P_{n-1}D^\lambda$ is parallel to $P_n E^\lambda$, $n \geqslant 2$, and the nth strip s_n is the curved-edge quadrilateral $P_{n-1}P_n E^\lambda D^\lambda$. The last P_N may locate outside of the edge $A_1^\lambda A_2^\lambda$ for which we simply let $P_N = A_2^\lambda$. This procedure constructs the total N strips $s_1, s_2, \ldots, s_N$, as shown by the left plot in Figure 3.1. Obviously, we have

$T^+_\lambda = \cup_{i=1}^N s_i$. Without loss of generality, we assume $\angle A^\lambda_3 E^\lambda D^\lambda \geqslant \angle A^\lambda_3 D^\lambda E^\lambda$, which implies

$$|P_{N-1}P_{N-2}| \geqslant |P_{N-2}P_{N-3}| \geqslant \cdots \geqslant |P_1 P_0| \geqslant l^\lambda \sin(\theta^\lambda) h_T, \tag{3.5}$$

where, in the last inequality, we have used the estimates (3.2a) and (3.2c). Therefore, we have $N \leqslant \frac{1}{l^\lambda \sin(\theta^\lambda)} + 1$, and this bound is independent of the interface. On each strip s_i, $i = 1, \dots, N-1$, i.e., the curved-edge quadrilateral $P_{i-1}P_i D^\lambda E^\lambda$, we consider a local system with the ξ-direction perpendicular to the parallel sides $P_{i-1}D^\lambda$ and $P_i E^\lambda$, and the η-direction perpendicular to the ξ-direction, as shown in the right plot in Figure 3.1. On this local system, let $f_1(\xi)$ and $f_2(\xi)$ be the functions of the line $P_{i-1}P_i$ and the curve $D^\lambda E^\lambda$, $\xi \in (0, \xi_i)$, respectively. Then the 1D Friedrichs inequality [1] yields

$$\|w\|^2_{L^2(s_i)} = \int_0^{\xi_i} \int_{f_1(\xi)}^{f_2(\xi)} w^2 d\eta d\xi \leqslant \int_0^{\xi_i} |f_2(\xi) - f_1(\xi)|^2 \int_{f_1(\xi)}^{f_2(\xi)} (\partial_\eta w)^2 d\eta d\xi \leqslant h_T^2 |w|^2_{H^1(s_i)}. \tag{3.6}$$

The estimation on the last strip s_N can be shown similarly. Then (3.6) together with the bound of N gives

$$\|w\|_{L^2(T^+_\lambda)} \leqslant \sum_{i=1}^N \|w\|_{L^2(s_i)} \leqslant h_T \sum_{i=1}^N |w|_{H^1(s_i)} \leqslant N h_T |w|_{H^1(T^+_\lambda)}. \tag{3.7}$$

Therefore, following the argument based on the mathematical induction [1], we have

$$\|w\|_{L^2(T^+_\lambda)} \leqslant C N^{p-1} h_T^{p-1} |w|_{H^{p-1}(T^+_\lambda)}, \tag{3.8}$$

where the constant C only depends on the degree p. Finally, (3.3) follows from (3.4) and (3.8). ∎

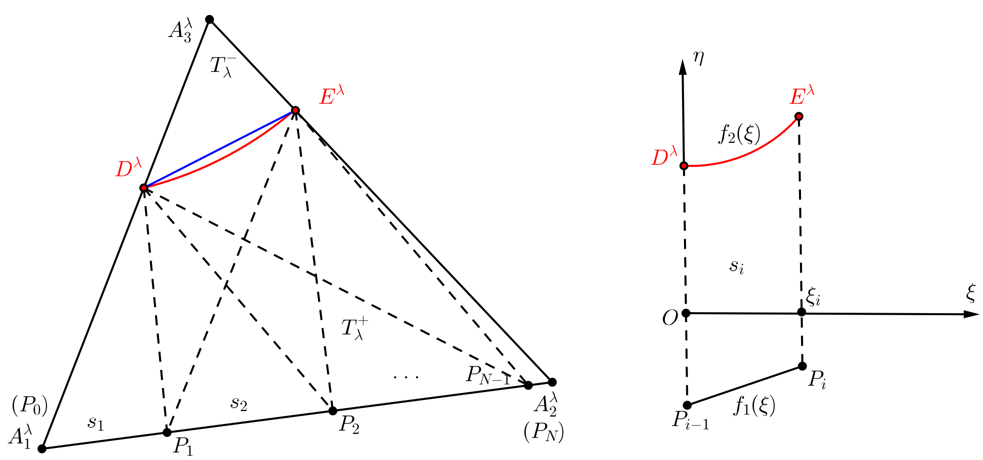

FIG. 3.1. *Interface elements and strips.*

Next, inspired by [51], we use Lemma 3.2 to establish a group of delicate norm equivalences on every interface element T and the related fictitious element T_λ. These results are the fundamental components in the proposed analysis framework. We begin with recalling the following lemma from [51].

LEMMA 3.4. *Given an integer $p \geqslant 0$ and $\mu \in (0,1)$, let K be a closed convex domain in $\mathbb{R}^2$ with a (piecewise) smooth boundary. Assume K' contains a homothetic subset of K with the scaling factor μ. Then there exists a constant $C(\mu, p+1)$ only depending on p and μ such that*

$$\|v\|_{L^2(K)} \leqslant C(\mu, p+1)\|v\|_{L^2(K')} \quad \forall v \in \mathbb{P}_p. \tag{3.9}$$

The following lemmas are about the equivalence of the L^2 norm on an interface element T and the related fictitious element T_λ.

LEMMA 3.5. *Given an interface element T and its fictitious element T_λ, for each degree p, there holds*

$$\|\cdot\|_{L^2(T)} \simeq \|\cdot\|_{L^2(T_\lambda)} \quad on\ \mathbb{P}_p. \tag{3.10}$$

Proof. By the definition, T is a homothetic subset of T_λ with the homothetic center being the incenter; hence (3.10) is a direct consequence of (3.9) by taking $\mu = 1/\lambda$. ∎

Now we define $\widetilde{T}^\pm_\lambda$ and $\widetilde{T}^\pm$ as the auxiliary straight-edge subelements partitioned by the line connecting the intersection points of the element boundary and the interface. In particular, on the interface element configuration shown by Figure 2.1, $\widetilde{T}^+_\lambda$ and $\widetilde{T}^-_\lambda$ are the straight-edge quadrilateral $A^\lambda_1 A^\lambda_2 E^\lambda D^\lambda$ and triangle $D^\lambda E^\lambda A^\lambda_3$, respectively, while $\widetilde{T}^+$ and $\widetilde{T}^-$ are the straight-edge quadrilateral A_1A_2ED and triangle DEA_3, respectively. Then, we have the following norm equivalence.

LEMMA 3.6. *Given an interface element T as shown in Figure* A.4*, for every degree p, if $|A_3D| \geqslant 1/2|A_3A_1|$ and $|A_3E| \geqslant 1/2|A_3A_2|$, there holds*

$$\|\cdot\|_{L^2(T^-)} \simeq \|\cdot\|_{L^2(\widetilde{T}^-)} \simeq \|\cdot\|_{L^2(T)} \quad on\ \mathbb{P}_p. \tag{3.11}$$

On the other hand, if $|A_3D| \leqslant 1/2|A_3A_1|$ or $|A_3E| \leqslant 1/2|A_3A_2|$, then there holds

$$\|\cdot\|_{L^2(T^+)} \simeq \|\cdot\|_{L^2(\widetilde{T}^+)} \simeq \|\cdot\|_{L^2(T)} \quad on\ \mathbb{P}_p. \tag{3.12}$$

Proof. See Appendix A.2. ∎

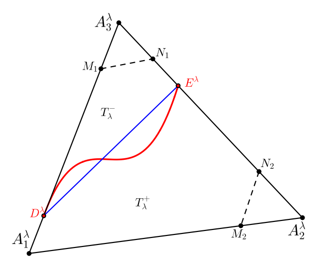

FIG. 3.2. *Equivalent norms on T^λ.*

LEMMA 3.7. *Given a fictitious element T_λ, $\lambda > 1$, as shown in Figure* 3.2*, associated with an interface element T, then for each degree p, there holds*

$$\|\cdot\|_{L^2(T^-_\lambda)} \simeq \|\cdot\|_{L^2(\widetilde{T}^-_\lambda)} \simeq \|\cdot\|_{L^2(T^+_\lambda)} \simeq \|\cdot\|_{L^2(\widetilde{T}^+_\lambda)} \simeq \|\cdot\|_{L^2(T_\lambda)} \quad on\ \mathbb{P}_p. \tag{3.13}$$

Proof. Using (3.2b) and the arguments used in Lemma 3.6, we can show that there always exist two fixed triangles $\triangle A_3^\lambda M_1 N_1 \subseteq T_\lambda^- \cap \widetilde{T}_\lambda^-$ and $A_2^\lambda M_2 N_2 \subseteq T_\lambda^+ \cap \widetilde{T}_\lambda^+$ both homothetic to T_λ regardless of the interface location, as shown in Figure 3.2. Then, (3.13) follows from similar arguments used for (A.3). ∎

Finally, we present the trace and inverse inequalities related to curved-edge subelements.

LEMMA 3.8. *Given each interface element T, on its fictitious element T_λ, for every $v \in \mathbb{P}_p$, the following hold:*

$$\text{the inverse inequality:} \quad \|\nabla v\|_{L^2(T_\lambda^\pm)} \lesssim h_T^{-1} \|v\|_{L^2(T_\lambda^\pm)}, \tag{3.14a}$$

$$\text{the trace inequality:} \quad \|v\|_{L^2(\Gamma_T^\lambda)} \lesssim h_T^{-1/2} \|v\|_{L^2(T_\lambda^\pm)}. \tag{3.14b}$$

Proof. For (3.14a), we apply Lemma 3.7 and the standard inverse inequality on T_λ to obtain

$$\|\nabla v\|_{L^2(T_\lambda^\pm)} \lesssim \|\nabla v\|_{L^2(T_\lambda)} \lesssim h_T^{-1} \|v\|_{L^2(T_\lambda)} \lesssim h_T^{-1} \|v\|_{L^2(T_\lambda^\pm)}. \tag{3.15}$$

For (3.14b), the standard inverse inequality on T_λ, Lemma 3.2 in [51], and Lemma 3.7 together lead to

$$\|v\|_{L^2(\Gamma_T^\lambda)} \lesssim h_T^{-1/2} \|v\|_{L^2(T_\lambda)} + h_T^{1/2} \|\nabla v\|_{L^2(T_\lambda)} \lesssim h_T^{-1/2} \|v\|_{L^2(T_\lambda)} \lesssim h_T^{-1/2} \|v\|_{L^2(T_\lambda^\pm)}. \tag{3.16}$$
∎

4. The Cauchy mapping.

To construct an IFE function is to find two polynomial components $z^-, z^+ \in \mathbb{P}_p$ such that, ideally, they satisfy all the jump conditions (1.1c)–(1.1e). In particular, according to the extended jump conditions in (1.1e), these two polynomials should satisfy $\beta^- \triangle z^- = \beta^+ \triangle z^+$. This consideration suggests one way to construct an IFE function: choose one of its polynomial components z^+, for instance, and then find the other polynomial component z^- of the IFE function by solving the following local Cauchy problem [27] imposed on the sub-fictitious-element T_λ^-:

$$\begin{aligned} \triangle z^- &= \frac{\beta^+}{\beta^-} \triangle z^+ && \text{in } T_\lambda^-, \\ z^- &= z^+ && \text{on } \Gamma_T^\lambda, \\ \nabla z^- \cdot \mathbf{n} &= \frac{\beta^+}{\beta^-} \nabla z^+ \cdot \mathbf{n} && \text{on } \Gamma_T^\lambda. \end{aligned}$$

We note that it is in general impossible to find a polynomial solution z^- to this Cauchy problem. Alternatively, in the proposed framework, we consider solving this Cauchy problem in an approximation sense based on the least squares finite element idea [10, 33], and this procedure further allows us to introduce a mapping which is a crucial tool in both the construction and analysis for pth degree IFE functions.

On each fictitious element T_λ associated with an interface element $T \in \mathcal{T}_h^i$, we introduce the following bilinear forms and the associated seminorms:

$$a_\lambda(v, w) = \int_{T_\lambda^-} \triangle v \triangle w dX + h_T^{-3} \int_{\Gamma_T^\lambda} vw ds + h_T^{-1} \int_{\Gamma_T^\lambda} \partial_{\mathbf{n}} v \, \partial_{\mathbf{n}} w ds \quad \forall v, w \in H^2(T_\lambda^-), \tag{4.1a}$$

(4.1b)

$$b_\lambda(v,w) = \int_{T_\lambda^-} \frac{\beta^+}{\beta^-} \triangle v \triangle w dX + h_T^{-3} \int_{\Gamma_T^\lambda} vwds + h_T^{-1} \int_{\Gamma_T^\lambda} \frac{\beta^+}{\beta^-} \partial_{\mathbf{n}} v \, \partial_{\mathbf{n}} w ds \;\forall v, w \in H^2(T_\lambda^-),$$

(4.1c)

$$|||v|||_{a_\lambda}^2 = a_\lambda(v,v), \qquad |||v|||_{b_\lambda}^2 = b_\lambda(v,v) \quad \forall v \in H^2(T_\lambda^-).$$

Here and from now on, we employ the notation $\partial_{\boldsymbol{\xi}} v = \nabla v \cdot \boldsymbol{\xi}$ for any direction $\boldsymbol{\xi}$. Recall the assumption that $\beta^- \geqslant \beta^+$; so

$$\frac{\beta^+}{\beta^-} |||v|||_{a_\lambda}^2 \leqslant |||v|||_{b_\lambda}^2 \leqslant |||v|||_{a_\lambda}^2 \quad \forall v \in \mathbb{P}_p. \tag{4.2}$$

The next lemma shows that the seminorms (4.1c) actually become norms when restricted on polynomial spaces.

LEMMA 4.1. *$|||\cdot|||_{a_\lambda}$ and $|||\cdot|||_{b_\lambda}$ are both norms on the polynomial space $\mathbb{P}_p$ for each degree $p \geq 1$.*

Proof. From (4.2), we only need to prove $|||\cdot|||_{a_\lambda}$ is a norm. The result for the linear case, i.e., $p = 1$, is trivial. Now we proceed by mathematical induction. Suppose the result is true for degree p. Then, given each $v \in \mathbb{P}_{p+1}$, $|||v|||_{a_\lambda} = 0$ is equivalent to $\triangle v \equiv 0$ and $v = 0$, $\partial_{\mathbf{n}} v = 0$ on Γ_T^λ. According to [25, 37], we actually have $\partial_{\mathbf{t}}^l v = 0$ for $l = 1, 2$, $\partial_{\mathbf{n}}^2 v = 0$, and $\partial_{\mathbf{n}} \partial_{\mathbf{t}} v = 0$ on Γ_T^λ where $\mathbf{t}$ is the tangential vector to Γ_T^λ. Consider the polynomial $\partial_x v \in \mathbb{P}_p$ and let $a\mathbf{n} + b\mathbf{t} = (1,0)^T$ on Γ_T^λ. Note that $\triangle v \equiv 0$ yields $\triangle \partial_x v \equiv 0$. Besides, since $\partial_{\mathbf{n}} v = \partial_{\mathbf{t}} v = 0$ on Γ_T^λ, we have $\partial_x v = a\partial_{\mathbf{n}} v + b\partial_{\mathbf{t}} v = 0$ on Γ_T^λ. In addition, there also holds $\partial_{\mathbf{n}} \partial_x v = a\partial_{\mathbf{n}}^2 v + b\partial_{\mathbf{n}} \partial_{\mathbf{t}} v = 0$ on Γ_T^λ. Therefore, by the hypothesis, we have $\partial_x v = 0$, and similarly $\partial_y v = 0$. Then v must be a constant. Now using $v = 0$ on Γ_T^λ, we have $v \equiv 0$. ∎

Based on Lemma 4.1, we can further prove an equivalence between the standard L^2 norm and $|||\cdot|||_{a_\lambda}$.

LEMMA 4.2. *Given every T_λ, $\lambda > 1$, associated with a $T \in \mathcal{T}_h^i$, there holds $h_T^2 |||\cdot|||_{a_\lambda} \simeq \|\cdot\|_{L^2(T_\lambda^-)}$ on $\mathbb{P}_p$.*

Proof. See Appendix A.3. ∎

Since $|||\cdot|||_{a_\lambda}$ is indeed a norm, the coercivity and boundedness of the bilinear form $a_\lambda(v,w)$ (Lemma 4.2 in [33]) under this special norm together with the Lax–Milgram theorem directly imply that for each $v \in \mathbb{P}_p$, there exists a unique $\tilde{v} \in \mathbb{P}_p$ satisfying the variational equation $a_\lambda(\tilde{v}, w) = b_\lambda(v,w)$ $\forall w \in \mathbb{P}_p$. According to the discussions in [33], computing $\tilde{v} \in \mathbb{P}_p$ for a given $v \in \mathbb{P}_p$ is related to solving a Cauchy problem weakly on T_λ^- with initial conditions imposed on Γ_T^λ, and this leads us to introduce a Cauchy mapping as follows.

DEFINITION 4.1. *Define a mapping $\mathfrak{C} : \mathbb{P}_p \to \mathbb{P}_p$ such that for every $v \in \mathbb{P}_p$, $\mathfrak{C}(v) \in \mathbb{P}_p$ is determined by*

$$a_\lambda(\mathfrak{C}(v), w) = b_\lambda(v,w) \quad \forall w \in \mathbb{P}_p, \tag{4.3}$$

and we call $\mathfrak{C}$ the Cauchy mapping.

Because of the uniqueness and the fact $\mathfrak{C}(0) = 0$, $\mathfrak{C}$ is a one-to-one (bijective) linear mapping from the polynomial space $\mathbb{P}_p$ to $\mathbb{P}_p$. In the following discussion, we let P_{T_λ} be the standard L^2 projection from $H^{p+1}(T_\lambda)$ onto the polynomial space

$\mathbb{P}_p$ on T_λ. The following properties of the *Cauchy mapping* $\mathfrak{C}$ are the fundamental ingredients for us to analyze the local approximation capability and trace inequalities of IFE spaces defined in section 5.

THEOREM 4.1. *For every $u \in PH^{p+1}(\Omega)$ with the extensions $u_E^\pm$, on each interface element T and its fictitious element T_λ, $\lambda > 1$, there holds*

$$\left\|\left|\mathfrak{C}(P_{T_\lambda}u_E^+) - P_{T_\lambda}u_E^-\right\|\right|_{a_\lambda} \lesssim h_T^{p-1}\left(|u_E^+|_{H^{p+1}(T_\lambda)} + |u_E^-|_{H^{p+1}(T_\lambda)}\right). \tag{4.4}$$

Proof. Let $w = \mathfrak{C}(P_{T_\lambda}u_E^+) - P_{T_\lambda}u_E^-$, and note that $w \in \mathbb{P}_p$, so the definition (4.3) directly yields

$$\begin{aligned}
\|w\|_{a_\lambda}^2 &= a_\lambda(\mathfrak{C}(P_{T_\lambda}u_E^+) - P_{T_\lambda}u_E^-, w) = b_\lambda(P_{T_\lambda}u_E^+, w) - a_\lambda(P_{T_\lambda}u_E^-, w) \\
&= \int_{T_\lambda^-}\left(\frac{\beta^+}{\beta^-}\triangle P_{T_\lambda}u_E^+ - \triangle P_{T_\lambda}u_E^-\right)\triangle w dX + h_T^{-3}\int_{\Gamma_T^\lambda}(P_{T_\lambda}u_E^+ - P_{T_\lambda}u_E^-)w ds \\
&\quad + h_T^{-1}\int_{\Gamma_T^\lambda}\left(\frac{\beta^+}{\beta^-}\partial_{\mathbf{n}}P_{T_\lambda}u_E^+ - \partial_{\mathbf{n}}P_{T_\lambda}u_E^-\right)\partial_{\mathbf{n}}w ds.
\end{aligned} \tag{4.5}$$

Then, applying Hölder's inequality to each term on the right-hand side of (4.5), we have

$$\begin{aligned}
\|w\|_{a_\lambda} \leqslant& \left\|\frac{\beta^+}{\beta^-}\triangle P_{T_\lambda}u_E^+ - \triangle P_{T_\lambda}u_E^-\right\|_{L^2(T_\lambda^-)} + h_T^{-3/2}\|P_{T_\lambda}u_E^+ - P_{T_\lambda}u_E^-\|_{L^2(\Gamma_T^\lambda)} \\
&+ h_T^{-1/2}\left\|\frac{\beta^+}{\beta^-}\partial_{\mathbf{n}}P_{T_\lambda}u_E^+ - \partial_{\mathbf{n}}P_{T_\lambda}u_E^-\right\|_{L^2(\Gamma_T^\lambda)}.
\end{aligned} \tag{4.6}$$

For the first term in (4.6), by the triangular inequality, the error estimate for the projection operator P_{T_λ}, and Lemma 3.3, we obtain

$$\begin{aligned}
&\left\|\frac{\beta^+}{\beta^-}\triangle P_{T_\lambda}u_E^+ - \triangle P_{T_\lambda}u_E^-\right\|_{L^2(T_\lambda^-)} \\
\leqslant& \left\|\frac{\beta^+}{\beta^-}\triangle P_{T_\lambda}u_E^+ - \frac{\beta^+}{\beta^-}\triangle u_E^+\right\|_{L^2(T_\lambda)} + \|\triangle P_{T_\lambda}u_E^- - \triangle u_E^-\|_{L^2(T_\lambda)} + \left\|\frac{\beta^+}{\beta^-}\triangle u_E^+ - \triangle u_E^-\right\|_{L^2(T_\lambda)} \\
\lesssim& \frac{\beta^+}{\beta^-}h_T^{p-1}|u_E^+|_{H^{p+1}(T_\lambda)} + h_T^{p-1}|u_E^-|_{H^{p+1}(T_\lambda)} + h_T^{p-1}\left(\frac{\beta^+}{\beta^-}|u_E^+|_{H^{p+1}(T_\lambda)} + |u_E^-|_{H^{p+1}(T_\lambda)}\right).
\end{aligned} \tag{4.7}$$

To estimate the second term in (4.6), we first apply the special trace inequality given by Lemma 3.2 in [51] and the error estimate for the projection operator P_{T_λ} to obtain

$$\begin{aligned}
\|P_{T_\lambda}u_E^\pm - u_E^\pm\|_{L^2(\Gamma_T^\lambda)} &\lesssim h_T^{-\frac{1}{2}}\|P_{T_\lambda}u_E^\pm - u_E^\pm\|_{L^2(T_\lambda)} + h_T^{\frac{1}{2}}\|\nabla(P_{T_\lambda}u_E^\pm - u_E^\pm)\|_{L^2(T_\lambda)} \\
&\lesssim h_T^{p+\frac{1}{2}}|u_E^\pm|_{H^{p+1}(T_\lambda)}.
\end{aligned} \tag{4.8}$$

Then, we employ the jump condition (1.1c) for $u_E^\pm$ to obtain

$$\begin{aligned}
h_T^{-3/2}\|P_{T_\lambda}u_E^+ - P_{T_\lambda}u_E^-\|_{L^2(\Gamma_T^\lambda)} \leqslant& h_T^{-3/2}(\|P_{T_\lambda}u_E^+ - u_E^+\|_{L^2(\Gamma_T^\lambda)} + \|P_{T_\lambda}u_E^- - u_E^-\|_{L^2(\Gamma_T^\lambda)}) \\
\lesssim& h_T^{p-1}(|u_E^+|_{H^{p+1}(T_\lambda)} + |u_E^-|_{H^{p+1}(T_\lambda)}).
\end{aligned} \tag{4.9}$$

By an argument similar to (4.8) and (4.9), we can also show that

$$h_T^{-1/2}\left\|\frac{\beta^+}{\beta^-}\partial_{\mathbf{n}}P_{T_\lambda}u_E^+ - \partial_{\mathbf{n}}P_{T_\lambda}u_E^-\right\|_{L^2(\Gamma_T^\lambda)} \lesssim \frac{\beta^+}{\beta^-}h_T^{p-1}|u_E^+|_{H^{p+1}(T_\lambda)} + h_T^{p-1}|u_E^-|_{H^{p+1}(T_\lambda)}. \tag{4.10}$$

Substituting (4.7), (4.9), and (4.10) into (4.6) yields the desired result. ∎

LEMMA 4.3. *On each interface element T and its fictitious element T_λ, $\lambda > 1$, the following hold:*

$$\|\!|\mathfrak{C}(v) - v|\!\|_{a_\lambda} \lesssim h_T^{-1}|v|_{H^1(T_\lambda^-)} \qquad \forall v \in \mathbb{P}_p, \tag{4.11a}$$

$$\|\!|\mathfrak{C}(v) - v|\!\|_{a_\lambda} \lesssim h_T^{-1}\frac{\beta^-}{\beta^+}|\mathfrak{C}(v)|_{H^1(T_\lambda^-)} \quad \forall v \in \mathbb{P}_p. \tag{4.11b}$$

Proof. Let $w = \mathfrak{C}(v) - v$. The definition (4.3), Hölder's inequality, and the assumption $\beta^- \geqslant \beta^+$ yield

$$\begin{aligned}
&\|\!|w|\!\|_{a_\lambda}^2 = a_\lambda(w,w) = b_\lambda(v,w) - a_\lambda(v,w)\\
&= \int_{T_\lambda^-}\left(\frac{\beta^+}{\beta^-} - 1\right)\triangle v\ \triangle w dX + h_T^{-1}\int_{\Gamma_T^\lambda}\left(\frac{\beta^+}{\beta^-} - 1\right)\partial_{\mathbf{n}}v\ \partial_{\mathbf{n}}w ds\\
&\leqslant \left(\|\triangle v\|_{L^2(T_\lambda^-)} + h_T^{-1/2}\|\partial_{\mathbf{n}}v\|_{L^2(\Gamma_T^\lambda)}\right)\|\!|w|\!\|_{a_\lambda} \lesssim h_T^{-1}|v|_{H^1(T_\lambda^-)}\|\!|w|\!\|_{a_\lambda},
\end{aligned} \tag{4.12}$$

which implies (4.11a), where in the last inequality above we have used the inverse inequality (3.14a) and trace inequality (3.14b). For (4.11b), by (4.2), we have

$$\|\!|w|\!\|_{a_\lambda}^2 \leqslant \frac{\beta^-}{\beta^+}\|\!|w|\!\|_{b_\lambda}^2 = \frac{\beta^-}{\beta^+}(b_\lambda(\mathfrak{C}(v),w) - a_\lambda(\mathfrak{C}(v),w)), \tag{4.13}$$

and the rest of the derivation is the same as (4.12). ∎

5. A *p*th degree IFE space. In this section, using the Cauchy mapping introduced in section 4, we proceed to define the pth degree IFE spaces and study their properties. Specifically, on each interface element $T \in \mathcal{T}_h^i$ with its fictitious element T_λ, $\lambda > 1$, the local pth degree IFE space is defined as a space of piecewise polynomials:

$$S_h^p(T) = \{v \in L^2(T)\ :\ \exists w \in \mathbb{P}_p \text{ s.t. } v|_{T^+} = w \text{ and } v|_{T^-} = \mathfrak{C}(w)\}. \tag{5.1}$$

By definition, every function in $S_h^p(T)$ is the extension of a polynomial from T^+ to T through the Cauchy mapping that enforces the jump conditions (1.1c) and (1.1d) across the interface naturally in a weak sense; hence, every function in this local pth degree IFE space is called a *Cauchy extension* of the related pth degree polynomial. On each noninterface element $T \in \mathcal{T}_h^n$, the local IFE space is simply a standard polynomial space, i.e., $S_h^p(T) = \mathbb{P}_p$. As usual, these local IFE spaces can be put together to form a global IFE space in the way suitable for a finite element method. For example, for the IFE method to be introduced in the next section, we can form the following global IFE space:

$$S_h^p(\Omega) = \{v \in L^2(\Omega)\ :\ v|_T \in S_h^p(T)\ \forall T \in \mathcal{T}_h \text{ and } v \text{ is continuous on each } e \in \mathcal{E}_h^n\}. \tag{5.2}$$

Alternatively, let $\{\zeta_i : i = 1, 2, \ldots, n\}$ be a set of basis functions with desirable features for the polynomial space $\mathbb{P}_p$ with $n = (p+1)(p+2)/2$. Clearly, since $\mathfrak{C}$ is bijective on

$\mathbb{P}_p$, the piecewise polynomials

$$v_i = \begin{cases} \zeta_i, & X \in T^+, \\ \mathfrak{C}(\zeta_i), & X \in T^-, \end{cases} \quad i = 1, 2, \dots, n, \quad \forall T \in \mathcal{T}_h^i \tag{5.3}$$

form a basis for the local IFE space $S_h^p(T)$; i.e., we have $S_h^p(T) = \mathrm{Span}\{v_i, 1 \le i \le n\}$.

Next, we show that the proposed IFE space (5.2) has the optimal approximation capability to the space $PH^{p+1}(\Omega)$ with respect to the polynomials used to construct the IFE space. On noninterface elements $T \in \mathcal{T}_h^n$, we simply consider the standard Lagrange type interpolation operator I_T [13]. The challenge is on interface elements where IFE functions are discontinuous across the interface Γ because of the lack of readily available error analysis tools in the literature. Inspired by [26], our contribution here is to introduce a new interpolation operator for gauging the approximation capability of the IFE space $S_h(T)$ on each interface element T. Recalling that P_{T_λ} is the standard L^2 projection from $H^{p+1}(T_\lambda)$ to $\mathbb{P}_p$, we define the following interpolation operator:

$$I_T u = \begin{cases} I_T^+ u := P_{T_\lambda} u_E^+ & \text{on } T^+, \\ I_T^- u := \mathfrak{C}(P_{T_\lambda} u_E^+) & \text{on } T^-, \end{cases} \quad \forall u \in PH^{p+1}(T_\lambda). \tag{5.4}$$

Then, the global interpolation operator $I_h \ : \ PH^{p+1}(\Omega) \to S_h^p(\Omega)$ is defined elementwisely as

$$I_h u|_T = I_T u \quad \forall T \in \mathcal{T}_h. \tag{5.5}$$

The key idea for using this interpolation operator to analyze the approximation capability of the proposed pth degree IFE space is a delicate decomposition of the interpolation errors illustrated by the diagram in Figure 5.1. As shown in this diagram, the error of the interpolation $I_T u$ can be decomposed into the error between the Sobolev extensions $u_E^s, s = \pm$, of the components of u and their projections $P_{T_\lambda} u_E^s, s = \pm$, and the error between the projection $P_{T_\lambda} u_E^-$ and the Cauchy extension $\mathfrak{C}(P_{T_\lambda} u_E^+)$. We note that the errors between the Sobolev extensions and their projections are well understood; hence, a solid arrow is used to connect them in the diagram. However, the difference between the projection $P_{T_\lambda} u_E^-$ and the Cauchy extension $\mathfrak{C}(P_{T_\lambda} u_E^+)$, connected by a dashed line in the diagram, is unknown in the literature, which motivates us to carry out preparations such as Theorem 4.1 in the previous sections.

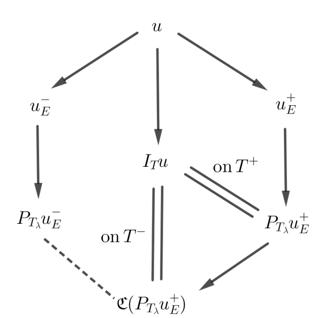

FIG. 5.1. *A decomposition of the interpolation error.*

The following theorem is about the optimal approximation capabilities of the proposed IFE space locally on each interface element.

THEOREM 5.1. *Let $u \in PH^{p+1}(\Omega)$. On every interface element $T \in \mathcal{T}_h^i$ with its associated fictitious element T_λ, $\lambda > 1$, the following estimates hold:*

$$\sum_{j=0}^{2} h_T^j |u_E^+ - I_T^+ u|_{H^j(T)} \lesssim h_T^{p+1} |u_E^+|_{H^{p+1}(T_\lambda)}, \tag{5.6a}$$

$$\sum_{j=0}^{2} h_T^j |u_E^- - I_T^- u|_{H^j(T)} \lesssim h_T^{p+1} \Big(|u_E^+|_{H^{p+1}(T_\lambda)} + |u_E^-|_{H^{p+1}(T_\lambda)} \Big), \tag{5.6b}$$

where $I_T^+ u$ and $I_T^- u$ are understood as polynomials on the whole element T.

Proof. We note that (5.6a) is simply the optimal approximation capability for the projection operator P_{T_λ}. For (5.6b), note that $I_T^- u - P_{T_\lambda} u_E^- = \mathfrak{C}(P_{T_\lambda} u_E^+) - P_{T_\lambda} u_E^- \in \mathbb{P}_p$; then the norm equivalence given in Lemmas 3.5, 3.7, and 4.2 together with the estimate given in Theorem 4.1 implies

$$\begin{aligned} \| I_T^- u - P_{T_\lambda} u_E^- \|_{L^2(T)} &\lesssim \| I_T^- u - P_{T_\lambda} u_E^- \|_{L^2(T_\lambda^-)} \lesssim h_T^2 \big\| \mathfrak{C}(P_{T_\lambda} u_E^+) - P_{T_\lambda} u_E^- \big\|_{a_\lambda} \\ &\lesssim h_T^{p+1} \Big(|u_E^+|_{H^{p+1}(T_\lambda)} + |u_E^-|_{H^{p+1}(T_\lambda)} \Big). \end{aligned} \tag{5.7}$$

In addition, applying the standard inverse inequality to (5.7), we have

$$h_T^j |I_T^- u - P_{T_\lambda} u_E^-|_{H^j(T)} \lesssim \| I_T^- u - P_{T_\lambda} u_E^- \|_{L^2(T)} \lesssim h_T^{p+1} \Big(|u_E^+|_{H^{p+1}(T_\lambda)} + |u_E^-|_{H^{p+1}(T_\lambda)} \Big). \tag{5.8}$$

Finally, the triangular inequality and the optimal approximation capability for the projection P_{T_λ} yield

$$\begin{aligned} h_T^j |u_E^- - I_T^- u|_{L^2(T)} &\leqslant h_T^j |u_E^- - P_{T_\lambda} u_E^-|_{L^2(T)} + h_T^j |P_{T_\lambda} u_E^- - I_T^- u|_{L^2(T)} \\ &\lesssim h_T^{p+1} \Big(|u_E^+|_{H^{p+1}(T_\lambda)} + |u_E^-|_{H^{p+1}(T_\lambda)} \Big). \end{aligned} \tag{5.9}$$ ∎

The following theorem provides an estimate for the global approximation capability in terms of the energy norm defined in (2.7b).

THEOREM 5.2. *Given each $u \in PH^{p+1}(\Omega)$, there holds*

$$\| u - I_h u \|_h \lesssim h^p \frac{\beta^-}{\sqrt{\beta^+}} \sum_{k=1}^{p+1} (|u^-|_{H^k(\Omega^-)} + |u^+|_{H^k(\Omega^+)}). \tag{5.10}$$

Proof. First, using the estimate for the Lagrange interpolation [13] on noninterface elements, we have

$$\sum_{T \in \mathcal{T}_h^n} \int_T \beta \| \nabla (u - I_T u) \|^2 dX \lesssim h^{2p} \beta^- \sum_{T \in \mathcal{T}_h^n} |u|^2_{H^{p+1}(T)}. \tag{5.11}$$

Over all the interface elements, Theorem 5.1 directly yields

$$\sum_{T \in \mathcal{T}_h^i} \int_T \beta \| \nabla (u - I_T u) \|^2 dX \lesssim h^{2p} \beta^- \sum_{T \in \mathcal{T}_h^i} (|u_E^+|^2_{H^{p+1}(T_\lambda)} + |u_E^-|^2_{H^{p+1}(T_\lambda)}). \tag{5.12}$$

In addition, given each interface edge $e \in \mathcal{E}_h^i$ with the two neighbor elements T^1 and T^2, let $e^\pm = e \cap \Omega^\pm$ and $\tilde{h} = \max\{h_{T^1}, h_{T^2}\}$. Using Theorem 5.1 and the standard trace inequality, we have

$$
\begin{aligned}
\sum_{r=\pm} \frac{\sigma_e^0 \gamma}{|e|} \int_{e^r} [u^r - I_h^r u]_e^2 ds &\lesssim \sum_{r=\pm} \tilde{h}^{-1} \gamma \int_e [u_E^r - I_h^r u]_e^2 ds \lesssim \sum_{r=\pm} \sum_{j=1,2} \tilde{h}^{-1} \gamma \int_e ((u_E^r - I_h^r u)|_{T^j})^2 ds \\
&\lesssim \sum_{r=\pm} \sum_{j=1,2} \gamma (\tilde{h}^{-2} \|u_E^r - I_{T^j}^r u\|_{L^2(T^j)}^2 + |u_E^r - I_{T^j}^r u|_{H^1(T^j)}^2) \\
&\lesssim \tilde{h}^{2p} \gamma (|u_E^+|_{H^{p+1}(T_\lambda^1 \cup T_\lambda^2)}^2 + |u_E^-|_{H^{p+1}(T_\lambda^1 \cup T_\lambda^2)}^2).
\end{aligned} \tag{5.13}
$$

The estimates on noninterface edges in $\mathcal{E}_h^i$ can be proved similarly. Thus, we have

$$
\sum_{e \in \mathcal{E}_h^i} \frac{\sigma_e^0 \gamma}{|e|} \int_e [u - I_h u]_e^2 ds \lesssim h^{2p} \gamma \sum_{T \in \mathcal{T}_h^i} (|u_E^+|_{H^{p+1}(T_\lambda)}^2 + |u_E^-|_{H^{p+1}(T_\lambda)}^2). \tag{5.14}
$$

Next, using Lemma 3.2 in [51], Theorem 5.1, and the standard trace inequality, we have

$$
\begin{aligned}
\sum_{T \in \mathcal{T}_h^i} \frac{\sigma_e^1 \gamma}{h_T} \int_{\Gamma_T} [u - I_h u]_\Gamma^2 ds &\lesssim \sum_{T \in \mathcal{T}_h^i} \sum_{r=\pm} h_T^{-1} \gamma \int_{\Gamma_T} (u_E^r - I_T^r u)^2 ds \\
&\lesssim \sum_{T \in \mathcal{T}_h^i} \sum_{r=\pm} h_T^{-1} \gamma \left(h_T^{-1} \|u_E^r - I_T^r u\|_{L^2(T)}^2 + h_T \|\nabla (u_E^r - I_T^r u)\|_{L^2(T)}^2 \right) \\
&\lesssim h_T^{2p} \gamma \sum_{T \in \mathcal{T}_h^i} (|u_E^+|_{H^{p+1}(T_\lambda)}^2 + |u_E^-|_{H^{p+1}(T_\lambda)}^2).
\end{aligned} \tag{5.15}
$$

By similar arguments, we can also show that

$$
\sum_{e \in \mathcal{E}_h^i} \frac{|e|}{\sigma_e^0 \gamma} \int_e (\{\beta \nabla (I_h u - u) \cdot \mathbf{n}_e\}_e)^2 ds \lesssim h^{2p} \gamma \sum_{T \in \mathcal{T}_h^i} (|u_E^+|_{H^{p+1}(T_\lambda^1 \cup T_\lambda^2)}^2 + |u_E^-|_{H^{p+1}(T_\lambda^1 \cup T_\lambda^2)}^2), \tag{5.16}
$$

$$
\sum_{T \in \mathcal{T}_h^i} \frac{h_T}{\sigma_e^1 \gamma} \int_{\Gamma_T} (\{\beta \nabla (I_h u - u) \cdot \mathbf{n}_\Gamma\}_\Gamma)^2 ds \lesssim h^{2p} \gamma \sum_{T \in \mathcal{T}_h^i} (|u_E^+|_{H^{p+1}(T_\lambda)}^2 + |u_E^-|_{H^{p+1}(T_\lambda)}^2). \tag{5.17}
$$

Now recall that $\gamma = (\beta^-)^2/\beta^+$ because of the assumption that $\beta^- \geq \beta^+$; then combining the estimations above and using the finite overlapping Assumption (A2), we arrive at

$$
|||u - I_h u|||_h \lesssim h^p \sqrt{\gamma} \left(|u_E^-|_{H^{p+1}(\Omega)} + |u_E^+|_{H^{p+1}(\Omega)} \right), \tag{5.18}
$$

which yields the desired result by the boundedness of the Sobolev extension in (2.9). □

Remark 5.1. Let $m \geqslant 1$ and $p \geqslant 1$ be two integers with $m \leqslant p$, $u \in PH^{m+1}(\Omega)$, and let I_h be the pth degree interpolation operator defined in (5.4). Using the more general approximation capability for the Lagrange interpolation operator and the standard L^2 projection operator, we can actually prove more general local estimates than (5.6),

$$
\sum_{j=0}^{2} h_T^j |u_E^+ - I_T^+ u|_{H^j(T)} \lesssim h_T^{m+1} |u_E^+|_{H^{m+1}(T_\lambda)}, \tag{5.19a}
$$

$$\sum_{j=0}^{2} h_T^j |u_E^- - I_T^- u|_{H^j(T)} \lesssim h_T^{m+1} \left(|u_E^+|_{H^{m+1}(T_\lambda)} + |u_E^-|_{H^{m+1}(T_\lambda)} \right), \tag{5.19b}$$

and a more general global estimate than (5.10),

$$|||u - I_h u|||_h \lesssim h^m \frac{\beta^-}{\sqrt{\beta^+}} \sum_{k=1}^{m+1} \left(|u^-|_{H^k(\Omega^-)} + |u^+|_{H^k(\Omega^+)} \right). \tag{5.20}$$

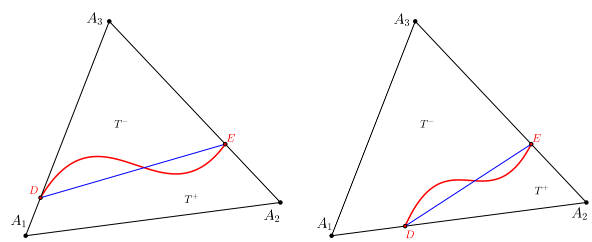

(a) Case 1 (b) Case 2

FIG. 5.2. *Trace inequalities on T.*

To finish this section, we establish a group of useful trace inequalities for the IFE functions on interface elements, which are critical for the error analysis in the next step. We emphasize that the trace inequalities for IFE functions as well as their proofs are nontrivial since the underlying macro polynomials do not have sufficient regularity for standard trace inequalities to hold. We need to seek new analysis techniques by taking advantage of the developed Cauchy extension, in particular Lemma 4.3, which shows that two polynomial components in an IFE function are restricted to behave collectively with each other in a certain way close to a standard polynomial. Now, without loss of generality, we consider the two interface element configurations as shown in Figure 5.2 where T^- is the triangular or quadrilateral curved-edge subelement. The analysis here, similar to that used in [23], highly relies on the trace inequalities for polynomials [52], which, for the reader's sake, we recall as follows: on every 2D triangle T,

$$\|v\|_{L^2(e)} \leqslant \sqrt{\frac{(k+1)(k+2)}{2}\frac{|e|}{|T|}}\|v\|_{L^2(T)} \quad \forall v \in \mathbb{P}_k(T), \quad e \text{ is an edge of } T. \tag{5.21}$$

THEOREM 5.3. *Let e be an edge of an interface element T in the configuration of Case 1 in Figure 5.2. If $|A_3D| \geqslant 1/2|A_3A_1|$ and $|A_3E| \geqslant 1/2|A_3A_2|$, then*

$$\|\beta\nabla\phi\|_{L^2(e)} \lesssim h_T^{-1/2}\|\beta\nabla\phi\|_{L^2(T)} \quad \forall \phi \in S_h^p(T). \tag{5.22}$$

On the other hand, if $|A_3D| \leqslant 1/2|A_3A_1|$ or $|A_3E| \leqslant 1/2|A_3A_2|$, then

$$\|\nabla\phi\|_{L^2(e)} \lesssim h_T^{-1/2}\|\nabla\phi\|_{L^2(T)} \quad \forall \phi \in S_h^p(T). \tag{5.23}$$

Proof. Without loss of generality, we consider the interface edge A_1A_3 and the noninterface edge A_1A_2. Recall that $\widetilde{T}^-$ and $\widetilde{T}^+$ are the straight-edge triangle $\triangle A_3DE$ and quadrilateral A_1A_2ED. First, if $|A_3E| \geqslant 1/2|A_3A_2|$ and $|A_3D| \geqslant 1/2|A_3A_1|$, the trace inequality (5.21) and the norm equivalence in (3.11) lead to

$$\|\beta^-\nabla\phi^-\|_{L^2(A_3D)} \lesssim h_T^{-1/2}\|\beta^-\nabla\phi^-\|_{L^2(\widetilde{T}^-)} \lesssim h_T^{-1/2}\|\beta^-\nabla\phi^-\|_{L^2(T^-)}. \tag{5.24}$$

For the estimation on the subedge DA_1, we apply the trace inequality (5.21) to obtain

$$\|\beta^+\nabla\phi^+\|_{L^2(DA_1)} \lesssim h_T^{-1/2}\|\beta^+\nabla\phi^+\|_{L^2(T)} \lesssim h_T^{-1/2}(\|\beta^+\nabla\phi^+\|_{L^2(T^+)}+\|\beta^+\nabla\phi^+\|_{L^2(T^-)}). \tag{5.25}$$

Now, using the fictitious element T_λ, we proceed to bound the second term on the right-hand side of (5.25). The triangular inequality and the norm equivalence in (3.10), (3.11), and (3.13) yield

$$\|\beta^+\nabla\phi^+\|_{L^2(T^-)} \lesssim \|\beta^+\nabla(\phi^+ - \phi^-)\|_{L^2(T_\lambda^-)} + \|\beta^-\nabla\phi^-\|_{L^2(T^-)}, \tag{5.26}$$

where we have also used the assumption $\beta^+ \leqslant \beta^-$. Recalling that $\phi^- = \mathfrak{C}(\phi^+)$, and using the inverse inequality (3.14a), the norm equivalence (3.10), (3.11), (3.13), Lemma 4.2, and (4.11b), we have

$$\begin{aligned}\|\beta^+\nabla(\phi^+ - \phi^-)\|_{L^2(T_\lambda^-)} &\lesssim h_T^{-1}\beta^+\|\phi^+ - \phi^-\|_{L^2(T_\lambda^-)} \lesssim h_T\beta^+ \left|\!\left|\!\left|\phi^+ - \mathfrak{C}(\phi^+)\right|\!\right|\!\right|_{a_\lambda}\\ &\lesssim \beta^-\|\nabla\mathfrak{C}(\phi^+)\|_{L^2(T_\lambda^-)} \lesssim \|\beta^-\nabla\phi^-\|_{L^2(T^-)}.\end{aligned} \tag{5.27}$$

Thus, combining (5.24)–(5.27), we have the desired trace inequality (5.22) on the interface edge $e = A_1A_3$. The estimation on the noninterface edge $e = A_1A_2$ follows from a derivation similar to (5.25)–(5.27).

Second, if $|A_3E| \leqslant 1/2|A_3A_2|$ or $|A_3D| \leqslant 1/2|A_3A_1|$, without loss of generality, we assume $|A_3D| \leqslant 1/2|A_3A_1|$. Then, the estimation on the subedge A_1D directly follows from the trace inequality (5.21) and the norm equivalence in (3.12). For the subedge A_3D, an argument similar to (5.25) and (5.26) yields

$$\begin{aligned}\|\nabla\phi^-\|_{L^2(A_3D)} \lesssim h_T^{-1/2}\|\nabla\phi^-\|_{L^2(T)} \lesssim h_T^{-1/2}(&\|\nabla(\phi^- - \phi^+)\|_{L^2(T_\lambda^+)} + \|\nabla\phi^+\|_{L^2(T^+)}\\ &+ \|\nabla\phi^-\|_{L^2(T^-)}).\end{aligned} \tag{5.28}$$

Then, similar to (5.27), but using (4.11a) here, we have

$$\begin{aligned}\|\nabla(\phi^- - \phi^+)\|_{L^2(T_\lambda^+)} &\lesssim h_T^{-1}\|\phi^- - \phi^+\|_{L^2(T_\lambda^+)} \lesssim h_T^{-1}\|\phi^- - \phi^+\|_{L^2(T_\lambda^-)} \lesssim h_T \left|\!\left|\!\left|\mathfrak{C}(\phi^+) - \phi^+\right|\!\right|\!\right|_{a_\lambda}\\ &\lesssim \|\nabla\phi^+\|_{L^2(T_\lambda^-)} \lesssim \|\nabla\phi^+\|_{L^2(T^+)}.\end{aligned} \tag{5.29}$$

Therefore, (5.23) on the interface edge A_1A_2 follows from (5.28)–(5.29). The result for the noninterface edge follows directly from the trace inequality (5.21) together with the norm equivalence (3.12). ∎

The next theorem concerns the trace inequalities on the interface.

THEOREM 5.4. *Let T be an interface element in the configuration of Case 1 in Figure 5.2. If $|A_3D| \geqslant 1/2|A_3A_1|$ and $|A_3E| \geqslant 1/2|A_3A_2|$, then*

$$\|\nabla\phi^-\|_{L^2(\Gamma_T)} \lesssim h_T^{-1/2}\|\nabla\phi^-\|_{L^2(T^-)},\ \|\beta^+\nabla\phi^+\|_{L^2(\Gamma_T)} \lesssim h_T^{-1/2}\|\beta\nabla\phi\|_{L^2(T)}\ \forall\phi\in S_h^p(T). \tag{5.30}$$

On the other hand, if $|A_3D| \leqslant 1/2|A_3A_1|$ or $|A_3E| \leqslant 1/2|A_3A_2|$, then

$$\|\nabla\phi^-\|_{L^2(\Gamma_T)} \lesssim h_T^{-1/2}\|\nabla\phi\|_{L^2(T)}, \quad \|\nabla\phi^+\|_{L^2(\Gamma_T)} \lesssim h_T^{-1/2}\|\nabla\phi^+\|_{L^2(T^+)} \quad \forall\phi\in S_h^p(T). \tag{5.31}$$

Proof. The proof is basically the same as that of Theorem 5.3. Here, for simplicity, we only discuss the case that $|A_3D| \geqslant 1/2|A_3A_1|$ and $|A_3E| \geqslant 1/2|A_3A_2|$, and the other case can be discussed similarly. The trace inequality (3.14b) and the norm equivalence in (3.10), (3.11), and (3.13) yield

$$\|\nabla\phi^-\|_{L^2(\Gamma_T)} \lesssim h_T^{-1/2}\|\nabla\phi^-\|_{L^2(T_\lambda^-)} \lesssim h_T^{-1/2}\|\nabla\phi^-\|_{L^2(T^-)}, \tag{5.32}$$

$$\|\beta^+\nabla\phi^+\|_{L^2(\Gamma_T)} \lesssim h_T^{-1/2}\|\beta^+\nabla\phi^+\|_{L^2(T_\lambda)} \lesssim h_T^{-1/2}(\|\beta^+\nabla\phi^+\|_{L^2(T^+)} + \|\beta^+\nabla\phi^+\|_{L^2(T^-)}). \tag{5.33}$$

Note that (5.32) already gives the first inequality in (5.30). Applying the results from (5.26), (5.27) to the second term in the right-hand side of (5.33), we arrive at the second inequality in (5.30). ∎

To avoid redundancy, we now present the trace inequalities for Case 2 in Figure 5.2 without giving the detailed proof because the arguments are basically the same as Theorems 5.3 and 5.4.

THEOREM 5.5. *Let e be an edge of an interface element T in the configuration of Case 2 in Figure 5.2. If $|A_2D| \geqslant 1/2|A_2A_1|$ and $|A_2E| \geqslant 1/2|A_3A_2|$, then*

$$\|\nabla\phi\|_{L^2(e)} \lesssim h_T^{-1/2}\|\nabla\phi\|_{L^2(T)} \quad \forall\phi \in S_h^p(T). \tag{5.34}$$

On the other hand, if $|A_2D| \leqslant 1/2|A_2A_1|$ or $|A_2E| \leqslant 1/2|A_3A_2|$, then

$$\|\beta\nabla\phi\|_{L^2(e)} \lesssim h_T^{-1/2}\|\beta\nabla\phi\|_{L^2(T)} \quad \forall\phi \in S_h^p(T). \tag{5.35}$$

THEOREM 5.6. *Let T be an interface element in the configuration of Case 2 in Figure 5.2. If $|A_2D| \geqslant 1/2|A_2A_1|$ and $|A_2E| \geqslant 1/2|A_3A_2|$, then*

$$\|\nabla\phi^-\|_{L^2(\Gamma_T)} \lesssim h_T^{-1/2}\|\nabla\phi\|_{L^2(T)}, \quad \|\nabla\phi^+\|_{L^2(\Gamma_T)} \lesssim h_T^{-1/2}\|\nabla\phi^+\|_{L^2(T^+)} \quad \forall\phi \in S_h^p(T). \tag{5.36}$$

On the other hand, if $|A_2D| \leqslant 1/2|A_2A_1|$ or $|A_2E| \leqslant 1/2|A_3A_2|$, then

$$\|\nabla\phi^-\|_{L^2(\Gamma_T)} \lesssim h_T^{-1/2}\|\nabla\phi^-\|_{L^2(T^-)}, \ \|\beta^+\nabla\phi^+\|_{L^2(\Gamma_T)} \lesssim h_T^{-1/2}\|\beta\nabla\phi\|_{L^2(T)} \ \forall\phi \in S_h^p(T). \tag{5.37}$$

Remark 5.2. We can summarize Theorems 5.3–5.6 as follows so that they can be directly used later on:

$$|e|^{1/2}\|\beta\nabla\phi\|_{L^2(e)} \leqslant C_t\frac{\beta^-}{\sqrt{\beta^+}}\|\sqrt{\beta}\nabla\phi\|_{L^2(T)} \ \text{ and } \ h_T^{1/2}\|\beta\nabla\phi\|_{L^2(\Gamma_T)} \leqslant C_t\frac{\beta^-}{\sqrt{\beta^+}}\|\sqrt{\beta}\nabla\phi\|_{L^2(T)} \tag{5.38}$$

for each edge e of an interface element T, where C_t is a constant independent of interface location and $\beta^\pm$.

6. A pth degree IFE method for the interface problems.

In this section, we present a pth degree IFE method and proceed to show a priori error estimation. Based on the bilinear form in (2.6), we define the pth degree IFE solution to the interface problem (1.1a)–(1.1d) as $u_h \in S_h^p(\Omega) \cap V_h$ such that

$$a_h(u_h, v_h) = L_f(v_h) \quad \forall v_h \in S_h^p(\Omega) \cap V_h. \tag{6.1}$$

Following tradition, we call (6.1) the symmetric, nonsymmetric, and incomplete pth degree IFE method for $\epsilon_0 = \epsilon_1 = -1$, $\epsilon_0 = \epsilon_1 = 1$, and $\epsilon_0 = \epsilon_1 = 0$ in (2.6), respectively. Note that the bilinear form (2.6b) used in this method involves the penalties on edges in $\mathcal{E}_h^i$ and the interface itself, which distinguishes the proposed IFE method from the PPIFE method [43], where the penalties are only used on the interface edges, or the CutFEM [28], where the penalties are only enforced on the interface. This pth degree IFE method (6.1) is also related to the selective IFE method [31] and the IFE method in [26] sans the penalty on the interface. We begin the error estimation for this method by establishing a relationship between the energy norms $\|\cdot\|_h$ and $\vert\kern-0.25ex\vert\kern-0.25ex\vert\cdot\vert\kern-0.25ex\vert\kern-0.25ex\vert_h$ in (2.7).

LEMMA 6.1. *For sufficiently large σ_e^0 and σ_e^1, there holds $\sqrt{2}\|v\|_h \geqslant \vert\kern-0.25ex\vert\kern-0.25ex\vert v\vert\kern-0.25ex\vert\kern-0.25ex\vert_h$ $\forall v \in S_h^p(\Omega)$.*

Proof. Given each $e \in \mathcal{E}_h^i$, let T^1 and T^2 be the two elements sharing e. Then Hölder's inequality and the trace inequality (5.38) yield

$$\frac{|e|}{\sigma_e^0\gamma}\int_e (\{\beta\nabla v\cdot \mathbf{n}_e\}_e)^2 ds \leqslant \frac{C_t^2}{2\sigma_e^0}(\|\sqrt{\beta}\nabla v\|^2_{L^2(T^1)} + \|\sqrt{\beta}\nabla v\|^2_{L^2(T^2)}), \tag{6.2}$$

$$\frac{h_T}{\sigma_e^1\gamma}\int_{\Gamma_T} (\{\beta\nabla v\cdot \mathbf{n}_\Gamma\}_\Gamma)^2 ds \leqslant \frac{C_t^2}{\sigma_e^1}\|\sqrt{\beta}\nabla v\|^2_{L^2(T)}. \tag{6.3}$$

Hence, we have $\vert\kern-0.25ex\vert\kern-0.25ex\vert v\vert\kern-0.25ex\vert\kern-0.25ex\vert_h^2 \leqslant 2\|v\|_h^2$ $\forall v \in S_h^p(\Omega)$ for any $\sigma_e^0 \geq 3C_t^2/2$ and any $\sigma_e^1 \geq C_t^2$. ◻

The following two theorems establish the coercivity and continuity of the bilinear form $a_h(\cdot,\cdot)$.

THEOREM 6.1. *Assume that the constants σ_e^0 and σ_e^1 are large enough for the symmetric and incomplete pth degree IFE method or that they are just positive for the nonsymmetric pth degree IFE method; then there holds*

$$a_h(v,v) \geqslant \frac{1}{2}\|v\|_h^2 \quad \forall v \in S_h^p(\Omega)\cap V_h. \tag{6.4}$$

Proof. We note that

$$\begin{aligned} a_h(v,v) = &\sum_{T\in\mathcal{T}_h}\int_T \beta\nabla v\cdot\nabla v dX + (\epsilon_0 - 1)\sum_{e\in\mathcal{E}_h^i}\int_e \{\beta\nabla v\cdot\mathbf{n}_e\}_e[v]_e ds + \sum_{e\in\mathcal{E}_h^i}\frac{\sigma_e^0\gamma}{|e|}\int_e [v]_e^2 ds \\ &+ (\epsilon_1 - 1)\sum_{T\in\mathcal{T}_h^i}\int_{\Gamma_T}\{\beta\nabla v\cdot\mathbf{n}_\Gamma\}_\Gamma[v]_\Gamma ds + \sum_{T\in\mathcal{T}_h^i}\frac{\sigma_e^1\gamma}{h_T}\int_{\Gamma_T}[v]_\Gamma^2 ds. \end{aligned} \tag{6.5}$$

Thus, the result (6.4) is trivial for the nonsymmetric case because $\epsilon_1 = \epsilon_0 = 1$. For the other two, given each $e \in \mathcal{E}_h^i$, let T^1 and T^2 be the two elements sharing e; then the derivation in (6.2) and (6.3) gives

$$\left|(\epsilon_0 - 1)\int_e \{\beta\nabla v\cdot\mathbf{n}_e\}_e[v]_e ds\right| \leqslant \alpha(\|\sqrt{\beta}\nabla v\|^2_{L^2(T^1)} + \|\sqrt{\beta}\nabla v\|^2_{L^2(T^2)}) + \frac{C_t^2\gamma}{2\alpha|e|}\|[v]_e\|^2_{L^2(e)}, \tag{6.6}$$

$$\left|(\epsilon_1 - 1)\int_{\Gamma_T} \{\beta\nabla v\cdot\mathbf{n}_\Gamma\}_\Gamma[v]_\Gamma ds\right| \leqslant 2\alpha\|\sqrt{\beta}\nabla v\|^2_{L^2(T)} + \frac{C_t^2\gamma}{2\alpha h_T}\|[v]_\Gamma\|^2_{L^2(\Gamma_T)} \tag{6.7}$$

for $\alpha > 0$, where we have used Young's inequality. Substituting (6.6) and (6.7) into (6.5) yields

$$a_h(v,v) \geqslant \sum_{T\in\mathcal{T}_h} (1-5\alpha)\|\sqrt{\beta}\nabla v\|^2_{L^2(T)} + \left(\sigma_e^0 - \frac{C_t^2}{2\alpha}\right)\frac{\gamma}{|e|}\|[v]_e\|^2_{L^2(e)}$$
$$+ \left(\sigma_e^1 - \frac{C_t^2}{2\alpha}\right)\frac{\gamma}{h_T}\|[v]_\Gamma\|^2_{L^2(\Gamma_T)}. \tag{6.8}$$

Then, letting $\alpha = 1/10$, $\sigma_e^0 \geq 5C_t^2 + 1/2$, and $\sigma_e^1 \geq 5C_t^2 + 1/2$ in (6.8) leads to the desired (6.4). ∎

THEOREM 6.2. *For every $v, w \in V_h$, there holds*

$$a_h(v,w) \leqslant 7|||v|||_h |||w|||_h. \tag{6.9}$$

Proof. The result follows from applying Hölder's inequality on each term in the bilinear form (2.6b). ∎

The coercivity in terms of the energy norm $\|\cdot\|_h$ guarantees the existence and uniqueness of the IFE solution u_h to the pth degree IFE method (6.1). The fundamental error estimation for the pth degree IFE solution u_h is given in the following theorem.

THEOREM 6.3. *Let $u \in PH^{p+1}(\Omega)$ with the integer $p \geqslant 1$ be the exact solution to the interface problem* (1.1a)–(1.1d). *Assume that the mesh $\mathcal{T}_h$ is fine enough such that all the previous results hold, and assume that σ_e^0 and σ_e^1 are large enough such that Lemma* 6.1 *and Theorem* 6.1 *hold. Then the pth degree IFE solution u_h has the following error bound:*

$$|||u - u_h|||_h \lesssim \frac{\beta^-}{\sqrt{\beta^+}} h^p \sum_{k=1}^{p+1} (|u^-|_{H^k(\Omega^-)} + |u^+|_{H^k(\Omega^+)}). \tag{6.10}$$

Proof. Note that the exact solution u satisfies the weak formulation (2.6) for every $v \in V_h$. Then

$$a_h(u_h - I_h u, v) = a_h(u - I_h u, v) \quad \forall v \in S_h^p(\Omega) \cap V_h, \tag{6.11}$$

where $I_h u \in S_h^p(\Omega)$ is given by (5.5). Since $u_h - I_h u \in S_h^p(\Omega) \cap V_h$, Lemma 6.1 and Theorems 6.1 and 6.2 give

$$\begin{aligned} \frac{1}{4}|||u_h - I_h u|||_h^2 &\leqslant \frac{1}{2}\|u_h - I_h u\|_h^2 \leqslant a_h(u_h - I_h u, u_h - I_h u) \\ &= a_h(u - I_h u, u_h - I_h u) \leqslant 7|||u - I_h u|||_h |||u_h - I_h u|||_h, \end{aligned} \tag{6.12}$$

which yields $|||u_h - I_h u|||_h \lesssim |||u - I_h u|||_h$. Then, (6.12), the triangular inequality, and Theorem 5.2 together lead to

$$|||u - u_h|||_h \lesssim |||u - I_h u|||_h + |||I_h u - u_h|||_h \lesssim h^p \frac{\beta^-}{\sqrt{\beta^+}} \sum_{k=1}^{p+1} (|u^-|_{H^k(\Omega^-)} + |u^+|_{H^k(\Omega^+)}). \tag{6.13}$$

∎

Remark 6.1. The regularity result from [16, 26, 34] gives

$$\beta^- \sum_{k=1}^{p+1} |u^-|_{H^k(\Omega^-)} + \beta^+ \sum_{k=1}^{p+1} |u^+|_{H^k(\Omega^+)} \lesssim \|f\|_{H^{p-1}(\Omega)}. \tag{6.14}$$

Therefore, (6.10) implies

$$|||u - u_h|||_h \lesssim \frac{\beta^+ + \beta^-}{(\beta^+)^{3/2}} h^p \|f\|_{H^{p-1}(\Omega)}. \tag{6.15}$$

Finally, we follow the standard duality argument to estimate the error in the L^2 norm.

THEOREM 6.4. *Under the conditions of Theorem* 6.3*, there holds*

$$\|u - u_h\|_{L^2(\Omega)} \lesssim \frac{(\beta^+ + \beta^-)\beta^-}{(\beta^+)^2} h^{p+1} \sum_{k=1}^{p+1} (|u^-|_{H^k(\Omega^-)} + |u^+|_{H^k(\Omega^+)}). \tag{6.16}$$

Proof. Define an auxiliary function $z \in PH^2(\Omega)$ as the solution to the interface problem (1.1a)–(1.1d) with the right-hand side f replaced by the solution error $u - u_h \in L^2(\Omega)$. In particular, we let I_h be the pth degree interpolation defined in (5.5). Because $u - u_h \in V_h$ and $I_h z \in S_h^p(\Omega) \cap V_h$, we have $a_h(I_h z, u - u_h) = 0$. By the continuity in Theorem 6.2, we have

$$\|u - u_h\|^2_{L^2(\Omega)} = a_h(z, u - u_h) = a_h(z - I_h z, u - u_h) \lesssim |||z - I_h z|||_h |||u - u_h|||_h. \tag{6.17}$$

In addition, Remark 5.1 and the regularity (6.14) yield

$$|||z - I_h z|||_h \lesssim h \frac{\beta^-}{\sqrt{\beta^+}} \sum_{k=1}^{2} (|z^-|_{H^k(\Omega^-)} + |z^+|_{H^k(\Omega^+)}) \lesssim \frac{\beta^+ + \beta^-}{(\beta^+)^{3/2}} h \|u - u_h\|_{L^2(\Omega)}. \tag{6.18}$$

Finally, combining (6.17), (6.18), and (6.10), we arrive at (6.16). ∎

Remark 6.2. Similar to Remark 6.1, we also have

$$\|u - u_h\|_{L^2(\Omega)} \lesssim \frac{(\beta^+ + \beta^-)^2}{(\beta^+)^3} h^{p+1} \|f\|_{H^{p-1}(\Omega)}. \tag{6.19}$$

Remark 6.3. Let $m \geqslant 1$ and $p \geqslant 1$ be two integers with $m \leqslant p$, and further let the exact solution $u \in PH^{m+1}(\Omega)$. Based on Remark 5.1, we can derive the following estimates corresponding to (6.10) and (6.16), respectively, for u with low regularity:

$$|||u - u_h|||_h \lesssim \frac{\beta^-}{\sqrt{\beta^+}} h^m \sum_{k=1}^{m+1} (|u^-|_{H^k(\Omega^-)} + |u^+|_{H^k(\Omega^+)}), \tag{6.20a}$$

$$\|u - u_h\|_{L^2(\Omega)} \lesssim \frac{(\beta^+ + \beta^-)\beta^-}{(\beta^+)^2} h^{m+1} \sum_{k=1}^{m+1} (|u^-|_{H^k(\Omega^-)} + |u^+|_{H^k(\Omega^+)}). \tag{6.20b}$$

Their proofs are standard and similar to those in Theorems 6.3 and 6.4 but with the estimate in (5.20). Therefore, for solving problems whose exact solutions do not have the optimal regularities, the proposed higher degree IFE method behaves in the same way as standard higher degree finite element methods in the sense that the order of convergence of the finite element solution decreases as the regularity of the exact solution deteriorates.

To finish this section, we present some representative numerical results in Table 6.1 to demonstrate the convergence features of the pth degree IFE method. To generate these numerical results, we apply the pth degree IFE method with $p = 3$ to the example from [22] in which $\Omega = (-1, 1) \times (-1, 1)$ and the interface is a circle with the radius $\pi/6.28$; similar examples have been used in the literature [22, 26, 43, 4]. In this table, the first column contains the values of the integer N such that the mesh size of the Cartesian mesh used for these numerical results is $h = 2/N$, and e_h^0 and e_h^1 are the errors of the third degree IFE solution measured in the L^2 and H^1 norms, respectively. Here, $\beta^- = 1$, $\beta^+ = 10$ represent a moderate discontinuity in the coefficient, while $\beta^- = 1$, $\beta^+ = 1000$ are for a much larger discontinuity. The data in Table 6.1 clearly demonstrate an optimal convergence, and our numerical experiments with other configurations demonstrate similar optimal-convergence behavior.

Table 6.1
Errors in pth degree IFE solutions for $p = 3$.

	$\beta^- = 1$, $\beta^+ = 10$				$\beta^- = 1$, $\beta^+ = 1000$			
	e_h^0	order	e_h^1	order	e_h^0	order	e_h^1	order
20	4.24E-5	NA	5.01E-3	NA	1.19E-5	NA	1.33E-3	NA
30	8.20E-6	4.05	1.48E-3	3.01	2.36E-6	3.98	4.03E-4	2.94
40	2.57E-6	4.03	6.26E-4	2.99	7.91E-7	3.80	1.81E-4	2.78
50	1.04E-6	4.04	3.20E-4	3.01	3.21E-7	4.03	9.34E-5	2.97
60	5.02E-7	4.02	1.85E-4	2.99	1.57E-7	3.91	5.50E-5	2.91
70	2.70E-7	4.03	1.17E-4	3.00	8.49E-8	4.01	3.45E-5	3.02
80	1.58E-7	4.02	7.82E-5	3.00	4.98E-8	3.98	2.33E-5	2.93

Appendix A. Technical results. In this section, we present the proof of the two technical results.

A.1. Proof of Lemma 3.2. First, in order to show (3.2a), we consider the auxiliary angle $\angle A_3^\lambda D^\lambda D$, as shown by Figure A.1. Denote the normal vectors to $D^\lambda E^\lambda$ and $D^\lambda D$ by $\bar{\mathbf{n}}$ and $\bar{\mathbf{n}}_0$. By geometry and (3.1b), there holds

$$\cos(\angle A_3^\lambda D^\lambda E^\lambda - \angle A_3^\lambda D^\lambda D) = \bar{\mathbf{n}} \cdot \bar{\mathbf{n}}_0 \geqslant 1 - \delta_1 \lambda^2 h_T^2. \tag{A.1}$$

We note that the smallest case for $\angle A_3^\lambda D^\lambda D$ is $\angle A_3^\lambda A_1^\lambda A_3$ directly calculated by

$$\begin{aligned} \angle A_3^\lambda A_1^\lambda A_3 &= \tan^{-1}\left(\frac{\lambda - 1}{\lambda \cot(\angle A_3^\lambda A_1^\lambda A_1) + \cot(\angle A_3 A_3^\lambda A_1^\lambda)}\right) \\ &\geqslant \tan^{-1}\left(\frac{\lambda - 1}{\lambda + 1}\tan(\theta_m/2)\right) := \theta_0, \end{aligned} \tag{A.2}$$

which only depends on λ and the shape regularity (2.3). So (A.1) and (A.2) yield

$$\angle A_3^\lambda D^\lambda E^\lambda \geqslant \angle A_3^\lambda D^\lambda D - \cos^{-1}(1 - \delta_1 \lambda^2 h^2) \geqslant \theta_0 - 2\sqrt{\delta_1}\lambda h_T,$$

which can be lower bounded by a positive constant independent of the interface location for h_T small enough. The argument for the angles $\angle A_3^\lambda E^\lambda D^\lambda$, θ_D, and θ_E is similar.

Next, for (3.2b), we consider the auxiliary line connecting D and E which intersects the lines $A_1^\lambda A_3^\lambda$ and $A_2^\lambda A_3^\lambda$ at D_0^λ and E_0^λ, respectively. See Figure A.2 for an illustration. From (3.1a) and (3.1b), it can be directly verified that the distance from E_0^λ to the line $D^\lambda E^\lambda$ is bounded by $(\delta_0 \lambda^2 + \sqrt{2\delta_1}\lambda)h_T^2$. Then (3.2a) yields

$|E^\lambda E_0^\lambda| \leqslant (\delta_0\lambda^2 + \sqrt{2\delta_1}\lambda)h_T^2/\sin(\theta^\lambda) := d_M h_T^2$, and so does $|D^\lambda D_0^\lambda|$. In addition, we let D_1^λ and E_1^λ be the intersection points of the edges A_1A_3 with $A_1^\lambda A_2^\lambda$ and $A_3^\lambda A_2^\lambda$, respectively. We define D_2^λ and E_2^λ similarly, as shown by Figure A.2. Without loss of generality, we assume $|A_3^\lambda E_0^\lambda|/|A_3^\lambda A_2^\lambda| \leqslant |A_3^\lambda D_0^\lambda|/|A_3^\lambda A_1^\lambda|$. Then E_0^λ must be between E_1^λ and E_2^λ. Hence, it can be verified that $\frac{|A_3^\lambda E_2^\lambda|}{|A_3^\lambda A_2^\lambda|} \leqslant \frac{\sigma\lambda+1}{\sigma\lambda+\lambda}$ and $\frac{|A_3^\lambda E_1^\lambda|}{|A_3^\lambda A_2^\lambda|} \geqslant \frac{\lambda-1}{\sigma\lambda+\lambda}$. Therefore, we have

$$\min\left\{\frac{|A_3^\lambda E^\lambda|}{|A_3^\lambda A_2^\lambda|}, \frac{|A_3^\lambda D^\lambda|}{|A_3^\lambda A_1^\lambda|}\right\} \leqslant \min\left\{\frac{|A_3^\lambda E_0^\lambda|}{|A_3^\lambda A_2^\lambda|}, \frac{|A_3^\lambda D_0^\lambda|}{|A_3^\lambda A_1^\lambda|}\right\} + \frac{d_M h_T^2}{\rho_T} \leqslant \frac{\sigma\lambda+1}{\sigma\lambda+\lambda} + d_M\sigma h_T,$$

$$\min\left\{\frac{|A_3^\lambda E^\lambda|}{|A_3^\lambda A_2^\lambda|}, \frac{|A_3^\lambda D^\lambda|}{|A_3^\lambda A_1^\lambda|}\right\} \geqslant \min\left\{\frac{|A_3^\lambda E_0^\lambda|}{|A_3^\lambda A_2^\lambda|}, \frac{|A_3^\lambda D_0^\lambda|}{|A_3^\lambda A_1^\lambda|}\right\} - \frac{d_M h_T^2}{\rho_T} \geqslant \frac{\lambda-1}{\sigma\lambda+\lambda} - d_M\sigma h_T.$$

which can be both upper bounded from 1 and lower bounded from 0 for h_T small enough.

At last, for (3.2c), let $D_0^\lambda E_0^\lambda$ be the segment parallel to $D^\lambda E^\lambda$ passing through D, as shown by Figure A.3. It is easy to verify that the shortest length of $D_0^\lambda E_0^\lambda$ is achieved when it is orthogonal to $A_3A_3^\lambda$ and passing through A_3, i.e., it moves to $D_3^\lambda E_3^\lambda$, as illustrated by Figure A.3. Therefore, using (3.1a), we have

$$|D^\lambda E^\lambda| \geqslant 2\tan(\angle A_3A_3^\lambda A_1^\lambda)(|A_3A_3^\lambda| - \delta_0\lambda^2 h_T^2) \geqslant 2\tan(\theta_m/2)\left(\frac{(\lambda-1)}{\sigma} - \delta_0\lambda^2 h_T\right)h_T \geqslant l^\lambda h_T$$

for some $l^\lambda > 0$ independent of interface location for h_T small enough, where we have used (2.2) and (2.3).

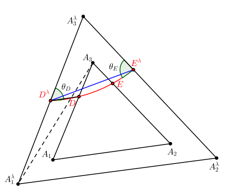

FIG. A.1. *Angle estimation.*

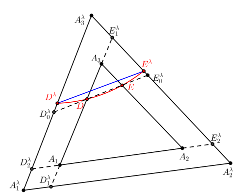

FIG. A.2. *Ratio estimation.*

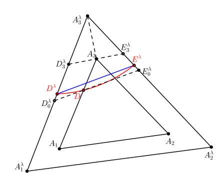

FIG. A.3. *Length estimation.*

A.2. Proof of Lemma 3.6. We first prove (3.11). Without of loss of generality, we consider the segment D_1E_1 which is parallel to the segment DE, tangent to Γ at a certain point and bounds Γ_T above. We further let M and N be the points on A_1A_3 and A_2A_3 such that $|A_3M|/|A_3A_1| = |A_3N|/|A_3A_2| = 1/3$; see the first plot in Figure A.4 for an illustration. Then $\triangle A_3MN$ is a homothetic subset of T with A_3 being the homothetic center and the scaling factor 1/3. Since $|A_3D| \geqslant 1/2|A_3A_1|$ and $|A_3E| \geqslant 1/2|A_3A_2|$, i.e., $\triangle A_3MN \subset \widetilde{T}^-$, given any $v \in \mathbb{P}_p$, Lemma 3.4 directly implies

$$\text{(A.3)}\quad \|v\|_{L^2(\widetilde{T}^-)} \leqslant \|v\|_{L^2(T)} \leqslant C(1/3, p+1)\|v\|_{L^2(\triangle A_3MN)} \leqslant C(1/3, p+1)\|v\|_{L^2(\widetilde{T}^-)},$$

which suggests $\|\cdot\|_{L^2(\widetilde{T}^-)} \simeq \|\cdot\|_{L^2(T)}$ on $\mathbb{P}_p$, where the constant $C(1/3, p+1)$ inherits from (3.9) with $\mu = 1/3$. In addition, we let d_1 and d_2 be the distance from A_3 to the lines DE and D_1E_1, respectively. Then, (3.1a) implies $|d_1 - d_2| \leqslant \delta_0 h_T^2$; hence we have $\frac{d_2}{d_1} = 1 - \frac{d_1-d_2}{d_1} \geqslant 1 - \frac{2\delta_0\sigma^2}{\pi}h_T \geqslant 2/3$ for h_T small enough, where we have also used

$d_0 \geqslant \frac{|\triangle A_1A_2A_3|}{2|DE|} \geqslant \frac{\pi\rho_T^2}{2h_T}$ and (2.2). Therefore, we can obtain $\frac{|A_3E_1|}{|A_3A_2|} = \frac{|A_3E_1|}{|A_3E|}\frac{|A_3E|}{|A_3A_2|} \geqslant 1/3$, and similarly $\frac{|A_3D_1|}{|A_3A_1|} \geqslant 1/3$. This shows $\triangle A_3MN \subseteq \triangle A_3D_1E_1 \subseteq T^- \subseteq T$. So the same argument as (A.3) yields $\|\cdot\|_{L^2(T^-)} \simeq \|\cdot\|_{L^2(T)}$ on $\mathbb{P}_p$, which further implies (3.11) together with (A.3).

Next, for (3.12), without loss of generality, we assume $|A_3E| \leqslant 1/2|A_3A_2|$. Let the points M and N be at the edges A_1A_2 and A_3A_2 such that $|A_2M|/|A_1A_2| = |A_2N|/|A_2A_3| = 1/3$; see the second plot in Figure A.4 for an illustration. Through similar arguments above, we can show $\triangle A_2NM \subseteq \widetilde{T}^+ \cap T^+$. Therefore, we have (3.12) by following the same arguments used for (A.3).

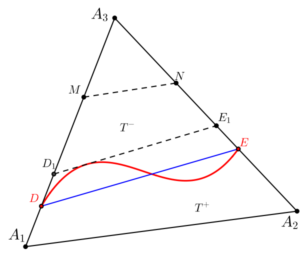

(a) Case 1

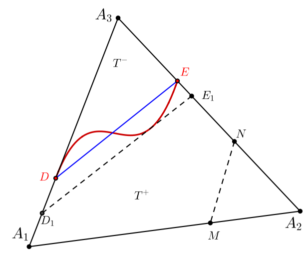

(b) Case 2

FIG. A.4. *Equivalent norms on T.*

A.3. Proof of Lemma 4.2. First, we consider the case that T^-_λ is the curved-edge triangular subelement $A_3^\lambda D^\lambda E^\lambda$, as shown in the left plot in Figure A.5. The first two estimates in (3.2a) enable us to construct an isosceles triangle $T_0 = \triangle PD^\lambda E^\lambda$ with $\angle PD^\lambda E^\lambda = \angle PE^\lambda D^\lambda = \theta^\lambda$ such that it is always contained in the straight-edge triangle $\triangle A_3^\lambda D^\lambda E^\lambda$. Then, we consider a special reference element $\hat{T}_0 = \triangle \hat{P}\hat{E}\hat{D}$ on the $\hat{x}$-$\hat{y}$ plane which is also isosceles with $\angle \hat{P}\hat{E}\hat{D} = \angle \hat{P}\hat{D}\hat{E} = \theta^\lambda$ and $|\hat{D}\hat{E}| = 1$ as shown in the second plot in Figure A.5. Define an affine mapping F which is simply a scaling rotation transformation:

(A.4)
$$F(\hat{x},\hat{y}) = |D^\lambda E^\lambda| \begin{bmatrix} \cos(\alpha) & -\sin(\alpha) \\ \sin(\alpha) & \cos(\alpha) \end{bmatrix} \begin{bmatrix} \hat{x} \\ \hat{y} \end{bmatrix} + D^\lambda, \text{ with } (l^\lambda)^2 h_T^2 \leqslant \left| \frac{\partial F(\hat{x},\hat{y})}{\partial(\hat{x},\hat{y})} \right| \leqslant \lambda^2 h_T^2,$$

where α is the angle between $D^\lambda E^\lambda$ and the x-axis, and the bound of Jacobian matrix follows from (3.2c).

Let F map a curve $\hat{\Gamma} : \hat{y} = f(\hat{x})$ to Γ^λ_T, and consider $\hat{v} = v(F(\hat{x},\hat{y})) \in \mathbb{P}_p$. Equations (A.4) and (3.1a) yield $|f(\hat{x})| \leqslant \delta_0(l^\lambda)^{-1}\lambda^2 h_T \ \forall \hat{x} \in (0,1)$. So, we can construct a new triangle $\hat{T}_1 = \triangle \hat{P}\hat{D}_1\hat{E}_1$ homothetic to $\hat{T}_0$ according to the center $\hat{P}$ with the scaling factor $|\hat{P}\hat{D}|/|\hat{P}\hat{D}_1| = |\hat{P}\hat{E}|/|\hat{P}\hat{E}_1| = 2/3$ such that it always contains the curve $\hat{\Gamma}$ inside for h_T small enough; see the right plot in Figure A.5 for an illustration. Then,

(A.5)
$$\begin{aligned}\|\hat{v}\|_{L^2(\hat{\Gamma})} &= \left(\int_0^1 \hat{v}^2(\hat{x}, f(\hat{x}))(1+f'^2(\hat{x}))^{1/2} d\hat{x} \right)^{1/2} \geqslant \left(\int_0^1 \left(\hat{v}(\hat{x},0) + \int_0^{f(\hat{x})} \partial_{\hat{y}} v d\hat{y} \right)^2 d\hat{x} \right)^{1/2} \\ &\geqslant \left(\int_0^1 \hat{v}^2(\hat{x},0)\hat{x} \right)^{1/2} - \left(\int_0^1 \left(\int_0^{f(\hat{x})} \partial_{\hat{y}} v d\hat{y} \right)^2 d\hat{x} \right)^{1/2}\end{aligned}$$

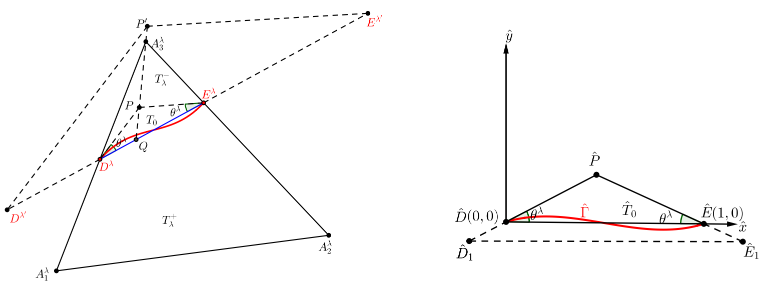

FIG. A.5. *Lemma* 4.2.

$$\geqslant \|\hat{v}\|_{L^2(0,1)} - (\delta_0/l^\lambda)^{1/2}\lambda h_T^{1/2}|\hat{v}|_{H^1(\hat{T}_1)},$$

where we have used Hölder's inequality and the bound for $|f(\hat{x})|$. From (3.1b), it is easy to verify that $|f'(\hat{x})| \leqslant 2\sqrt{2}\delta_1^{1/2}\lambda h_T \ \forall \hat{x} \in (0,1)$, for h_T small enough, which shows

(A.6)

$$\begin{aligned}\|\partial_{\mathbf{n}}\hat{v}\|_{\hat{\Gamma}} &= \left(\int_0^1 \left(-f'(\hat{x})\partial_{\hat{x}}\hat{v}(\hat{x}, f(\hat{x})) + \partial_{\hat{y}}\hat{v}(\hat{x}, f(\hat{x}))\right)^2 d\hat{x}\right)^{1/2} \\ &\geqslant \left(\int_0^1 (\partial_{\hat{y}}\hat{v}(\hat{x}, f(\hat{x})))^2 d\hat{x}\right)^{1/2} - 2\sqrt{2}\delta_1^{1/2}\lambda h_T \left(\int_0^1 (\partial_{\hat{x}}\hat{v}(\hat{x}, f(\hat{x})))^2 d\hat{x}\right)^{1/2}.\end{aligned}$$

Applying the similar arguments in (A.5) to each term in the right-hand side of (A.6), we obtain

$$\text{(A.7)} \qquad \left(\int_0^1 (\partial_{\hat{y}}\hat{v}(\hat{x}, f(\hat{x})))^2 d\hat{x}\right)^{1/2} \geqslant \|\partial_{\hat{y}}\hat{v}\|_{L^2(0,1)} - (\delta_0/l^\lambda)^{1/2}\lambda h_T^{1/2}|\hat{v}|_{H^2(\hat{T}_1)},$$

$$\text{(A.8)} \qquad \left(\int_0^1 (\partial_{\hat{x}}\hat{v}(\hat{x}, f(\hat{x})))^2 d\hat{x}\right)^{1/2} \leqslant \|\partial_{\hat{x}}\hat{v}\|_{L^2(0,1)} + (\delta_0/l^\lambda)^{1/2}\lambda h_T^{1/2}|\hat{v}|_{H^2(\hat{T}_1)}.$$

Substituting (A.7) and (A.8) into (A.6), and using the trace inequality (5.21) on $\|\partial_{\hat{x}}\hat{v}\|_{L^2(0,1)}$ in (A.8) together with the distance from $\hat{P}$ to $\hat{D}\hat{E}$ equaling $\tan(\theta^\lambda)/2$, we have

$$\text{(A.9)} \qquad \|\partial_{\mathbf{n}}\hat{v}\|_{\hat{\Gamma}} \geqslant \|\partial_{\hat{y}}\hat{v}\|_{L^2(0,1)} - \left[C_1 h_T|\hat{v}|_{H^1(\hat{T}_0)} + (C_2 h_T^{1/2} + C_3 h_T^{3/2})|\hat{v}|_{H^2(\hat{T}_1)}\right],$$

where C_1, C_2, C_3 depend only on p, λ, δ_1, δ_2, and θ^λ. Combining (A.5) and (A.9), using Lemma 3.4 to bound $|\hat{v}|_{H^k(\hat{T}_1)}$ by $|\hat{v}|_{H^k(\hat{T}_0)}$, $k = 1, 2$, with $\mu = 2/3$, and applying the inverse inequality on $\hat{T}_0$, we have

$$\|\triangle\hat{v}\|_{L^2(\hat{T}_0)} + \|\hat{v}\|_{L^2(\hat{\Gamma})} + \|\partial_{\mathbf{n}}\hat{v}\|_{L^2(\hat{\Gamma})} \geqslant \|\triangle\hat{v}\|_{L^2(\hat{T}_0)} + \|\hat{v}\|_{L^2(0,1)} + \|\partial_{\hat{y}}\hat{v}\|_{L^2(0,1)} - Ch_T^{1/2}\|\hat{v}\|_{L^2(\hat{T}_0)}$$

for h_T small enough, where the previous derivation shows this generic constant C also only depends on p, λ, δ_1, δ_2, and θ^λ. By the same argument in Lemma 4.1, $\|\triangle\hat{v}\|_{L^2(\hat{T}_0)} + \|\hat{v}\|_{L^2(0,1)} + \|\partial_{\hat{y}}\hat{v}\|_{L^2(0,1)}$ forms a norm on the polynomial space $\mathbb{P}_p$. Therefore, the norm equivalence on finite dimensional spaces yields

(A.10)

$$\|\triangle\hat{v}\|_{L^2(\hat{T}_0)} + \|\hat{v}\|_{L^2(\hat{\Gamma})} + \|\partial_{\mathbf{n}}\hat{v}\|_{L^2(\hat{\Gamma})} \geqslant C\|\hat{v}\|_{L^2(\hat{T}_0)} - Ch_T^{1/2}\|\hat{v}\|_{L^2(\hat{T}_0)} \geqslant C\|\hat{v}\|_{L^2(\hat{T}_0)}$$

for h_T small enough. Furthermore, Lemma 3.7 indicates $\|\triangle v\|_{L^2(T^-_\lambda)} \geqslant C\|\triangle v\|_{L^2(\widetilde{T}^-_\lambda)} \geqslant C\|\triangle v\|_{L^2(T_0)}$, where we recall $\widetilde{T}^-_\lambda = \triangle A^\lambda_3 D^\lambda E^\lambda$. Hence, using (A.10), (A.4), and the scaling argument, we arrive at

(A.11)

$$\begin{aligned}\|\!|v|\!\|^2_{a_\lambda} &\geqslant C\|\triangle v\|^2_{L^2(T_0)} + h_T^{-3}\|v\|^2_{L^2(\Gamma^\lambda_T)} + h_T^{-1}\|\partial_{\mathbf{n}} v\|^2_{L^2(\Gamma^\lambda_T)} \\ &\geqslant Ch_T^{-2}\left(\|\triangle \hat{v}\|^2_{L^2(\hat{T}_0)} + \|\hat{v}\|^2_{L^2(\hat{\Gamma})} + \|\partial_{\mathbf{n}}\hat{v}\|^2_{L^2(\hat{\Gamma})}\right) \geqslant Ch_T^{-2}\|\hat{v}\|^2_{L^2(\hat{T}_0)} \geqslant Ch_T^{-4}\|v\|^2_{L^2(T_0)}.\end{aligned}$$

Next, on T_λ, we consider the intersection point Q of the lines $A^\lambda_3 P$ and $D^\lambda E^\lambda$. By (3.2c), we have

(A.12)

$$\frac{|QP|}{|QA^\lambda_3|} = \frac{\sin(\theta^\lambda)|PE^\lambda|}{\sin(\angle A^\lambda_3 E^\lambda D^\lambda)|A^\lambda_3 E^\lambda|} = \frac{\sin(\theta^\lambda)|D^\lambda E^\lambda|}{2\cos(\theta^\lambda)\sin(\angle A^\lambda_3 E^\lambda D^\lambda)|A^\lambda_3 E^\lambda|} \geqslant \frac{\tan(\theta^\lambda) l^\lambda}{2\lambda}.$$

Therefore, we can construct a triangle $T'_0 = \triangle P' D^{\lambda'} E^{\lambda'}$ which is homothetic to T_0 according to the chosen center Q such that $|QP|/|QP'| = \frac{\tan(\theta^\lambda) l^\lambda}{4\lambda}$, i.e., a fixed scaling factor. Then, the triangle $\widetilde{T}^-_\lambda = \triangle A^\lambda_3 D^\lambda E^\lambda$ is always contained in T'_0 regardless of the interface location inside T_λ, as shown in Figure A.5. Hence, using Lemma 3.4 again, the equivalence norms in Lemma 3.7 and (A.11), for each $v \in \mathbb{P}_p$, we have

$$\|v\|_{L^2(T^-_\lambda)} \leqslant C\|v\|_{L^2(\widetilde{T}^-_\lambda)} \leqslant C\|v\|_{T'_0} \leqslant C\|v\|_{L^2(T_0)} \leqslant Ch_T^2\|\!|v|\!\|_{a_\lambda}.$$

The other direction $\|v\|_{L^2(T^-_\lambda)} \geqslant Ch_T^2\|\!|v|\!\|_{a_\lambda}$ can be easily obtained by the trace inequality and inverse inequality in Lemma 3.8.

Second, we note that Lemma 3.7 implies that $C_1\|\triangle v\|_{L^2(T^+_\lambda)} \leqslant \|\triangle v\|_{L^2(T^-_\lambda)} \leqslant C_2\|\triangle v\|_{L^2(T^+_\lambda)}$. Thus, when T^-_λ is the curved-edge quadrilateral subelement of T_λ, the result simply follows from what we have already shown for the curved-edge triangular subelement together with the norm equivalence in Lemma 3.7.

REFERENCES

[1] R. A. Adams and J. J. F. Fournier, *Sobolev Spaces*, 2nd ed., Pure Appl. Math. (Amsterdam) 140, Elsevier, London, Amsterdam, 2003.

[2] S. Adjerid, M. Ben-Romdhane, and T. Lin, *Higher degree immersed finite element methods for second-order elliptic interface problems*, Int. J. Numer. Anal. Model., 11 (2014), pp. 541–566.

[3] S. Adjerid, M. Ben-Romdhane, and T. Lin, *Higher degree immersed finite element spaces constructed according to the actual interface*, Comput. Math. Appl., 75 (2018), pp. 1868–1881.

[4] S. Adjerid, R. Guo, and T. Lin, *High degree immersed finite element spaces by a least squares method*, Int. J. Numer. Anal. Model., 14 (2016), pp. 604–626.

[5] S. Adjerid and T. Lin, *A p-th degree immersed finite element for boundary value problems with discontinuous coefficients*, Appl. Numer. Math., 59 (2009), pp. 1303–1321.

[6] M. Ainsworth and B. Senior, *An adaptive refinement strategy for hp-finite element computations*, Appl. Numer. Math., 26 (1998), pp. 165–178.

[7] I. Babuška and J. E. Osborn, *Generalized finite element methods: Their performance and their relation to mixed methods*, SIAM J. Numer. Anal., 20 (1983), pp. 510–536, https://doi.org/10.1137/0720034.

[8] I. Babuška, *The finite element method for elliptic equations with discontinuous coefficients*, Computing (Arch. Elektron. Rechnen), 5 (1970), pp. 207–213.

[9] I. Babuška, G. Caloz, and J. E. Osborn, *Special finite element methods for a class of second order elliptic problems with rough coefficients*, SIAM J. Numer. Anal., 31 (1994), pp. 945–981, https://doi.org/10.1137/0731051.

[10] P. B. Bochev and M. D. Gunzburger, *Least-Squares Finite Element Methods*, Appl. Math. Sci. 166, Springer, New York, 2009.

[11] D. Braess, *Finite Elements: Theory, Fast Solvers, and Applications in Solid Mechanics*, 2nd ed., Cambridge University Press, Cambridge, UK, 2001; translated from the 1992 German edition by L. L. Schumaker.

[12] J. H. Bramble and J. T. King, *A finite element method for interface problems in domains with smooth boundaries and interfaces*, Adv. Comput. Math., 6 (1996), pp. 109–138.

[13] S. C. Brenner and L. R. Scott, *The Mathematical Theory of Finite Element Methods*, 3rd ed., Texts Appl. Math. 15, Springer, New York, 2008.

[14] E. Burman, S. Claus, P. Hansbo, M. G. Larson, and A. Massing, *CutFEM: Discretizing geometry and partial differential equations*, Internat. J. Numer. Methods Engrg., 104 (2015), pp. 472–501.

[15] Z. Chen and J. Zou, *Finite element methods and their convergence for elliptic and parabolic interface problems*, Numer. Math., 79 (1998), pp. 175–202.

[16] C.-C. Chu, I. G. Graham, and T.-Y. Hou, *A new multiscale finite element method for high-contrast elliptic interface problems*, Math. Comp., 79 (2010), pp. 1915–1955.

[17] R. W. Clough and J. L. Tocher, *Finite element stiffness matrices for analysis of plate bending*, in Proceedings of the Conference on Matrix Methods in Structural Mechanics, Wright-Patterson Air Force Base, OH, 1966, pp. 515–545.

[18] J. Dolbow, N. Moës, and T. Belytschko, *An extended finite element method for modeling crack growth with frictional contact*, Comput. Methods Appl. Mech. Engrg., 190 (2001), pp. 6825–6846.

[19] Y. Efendiev and T. Y. Hou, *Multiscale Finite Element Methods: Theory and Applications*, Surveys Tutorials Appl. Math. Sci. 4, Springer, New York, 2009.

[20] D. Gilbarg and N. S. Trudinger, *Elliptic Partial Differential Equations of Second Order*, 2nd ed., Grundlehren Math. Wiss. 224, Springer, Berlin, 2001.

[21] Y. Gong, B. Li, and Z. Li, *Immersed-interface finite-element methods for elliptic interface problems with nonhomogeneous jump conditions*, SIAM J. Numer. Anal., 46 (2008), pp. 472–495, https://doi.org/10.1137/060666482.

[22] R. Guo and T. Lin, *A group of immersed finite element spaces for elliptic interface problems*, IMA J. Numer. Anal., 39 (2019), pp. 482–511.

[23] R. Guo, T. Lin, and Y. Lin, *A Partially Penalized Immersed Finite Element Method and Its Priori Error Estimations for Elasticity Interface Problems*, submitted, 2018.

[24] R. Guo, T. Lin, and X. Zhang, *Nonconforming immersed finite element spaces for elliptic interface problems*, Comput. Math. Appl., 75 (2018), pp. 2002–2016.

[25] J. Guzmán, M. A. Sánchez, and M. Sarkis, *Higher-order finite element methods for elliptic problems with interfaces*, ESAIM Math. Model. Numer. Anal., 50 (2016), pp. 1561–1583.

[26] J. Guzmán, M. A. Sánchez, and M. Sarkis, *A finite element method for high-contrast interface problems with error estimates independent of contrast*, J. Sci. Comput., 73 (2017), pp. 330–365.

[27] J. Hadamard, *Lectures on Cauchy's Problem in Linear Partial Differential Equations*, Dover, New York, 1952.

[28] A. Hansbo and P. Hansbo, *An unfitted finite element method, based on Nitsche's method, for elliptic interface problems*, Comput. Methods Appl. Mech. Engrg., 191 (2002), pp. 5537–5552.

[29] X. He, T. Lin, and Y. Lin, *Approximation capability of a bilinear immersed finite element space*, Numer. Methods Partial Differential Equations, 24 (2008), pp. 1265–1300.

[30] X. He, T. Lin, and Y. Lin, *Immersed finite element methods for elliptic interface problems with non-homogeneous jump conditions*, Int. J. Numer. Anal. Model., 8 (2011), pp. 284–301.

[31] X. He, T. Lin, and Y. Lin, *A selective immersed discontinuous Galerkin method for elliptic interface problems*, Math. Methods Appl. Sci., 37 (2014), pp. 983–1002.

[32] D. Holder, ed., *Electrical Impedance Tomography: Methods, History and Applications*, CRC Press, Boca Raton, FL, 2004.

[33] X. Hu, L. Mu, and X. Ye, *A simple finite element method of the Cauchy problem for Poisson equation*, Int. J. Numer. Anal. Model., 14 (2017), pp. 591–603.

[34] J. Huang and J. Zou, *Some new a priori estimates for second-order elliptic and parabolic interface problems*, J. Differential Equations, 184 (2002), pp. 570–586.

[35] F. B. Jensen, W. A. Kuperman, M. B. Porter, and H. Schmidt, *Wave propagation theory*, in Computational Ocean Acoustics, Springer, New York, 2011, pp. 65–153.

[36] C. Lehrenfeld, *A higher order isoparametric fictitious domain method for level set domains*, in Geometrically Unfitted Finite Element Methods and Applications, S. P. A. Borda et al., eds., Springer, Cham, 2018, pp. 65–92.

[37] R. J. LeVeque and Z. L. Li, *The immersed interface method for elliptic equations with discontinuous coefficients and singular sources*, SIAM J. Numer. Anal., 31 (1994), pp. 1019–1044, https://doi.org/10.1137/0731054.

[38] J. Li, J. M. Melenk, B. Wohlmuth, and J. Zou, *Optimal a priori estimates for higher order finite elements for elliptic interface problems*, Appl. Numer. Math., 60 (2010), pp. 19–37.

[39] Z. Li, T. Lin, Y. Lin, and R. C. Rogers, *An immersed finite element space and its approximation capability*, Numer. Methods Partial Differential Equations, 20 (2004), pp. 338–367.

[40] Z. Li and K. Ito, *The Immersed Interface Method: Numerical Solutions of PDEs Involving Interfaces and Irregular Domains*, Frontiers Appl. Math. 33, SIAM, Philadelphia, 2006, https://doi.org/10.1137/1.9780898717464.

[41] Z. Li, T. Lin, and X. Wu, *New Cartesian grid methods for interface problems using the finite element formulation*, Numer. Math., 96 (2003), pp. 61–98.

[42] T. Lin, Y. Lin, R. Rogers, and M. L. Ryan, *A rectangular immersed finite element space for interface problems*, in Scientific Computing and Applications (Kananaskis, AB, 2000), P. Minev and Y. Lin, eds., Adv. Comput. Theory Pract. 7, Nova Science, Huntington, NY, 2001, pp. 107–114.

[43] T. Lin, Y. Lin, and X. Zhang, *Partially penalized immersed finite element methods for elliptic interface problems*, SIAM J. Numer. Anal., 53 (2015), pp. 1121–1144, https://doi.org/10.1137/130912700.

[44] R. Massjung, *An unfitted discontinuous Galerkin method applied to elliptic interface problems*, SIAM J. Numer. Anal., 50 (2012), pp. 3134–3162, https://doi.org/10.1137/090763093.

[45] M. Medvinsky, S. Tsynkov, and E. Turkel, *Solving the Helmholtz equation for general smooth geometry using simple grids*, Wave Motion, 62 (2016), pp. 75–97.

[46] J. M. Melenk and I. Babuška, *The partition of unity finite element method: Basic theory and applications*, Comput. Methods Appl. Mech. Engrg., 139 (1996), pp. 289–314.

[47] Y. Renardy and M. Renardy, *PROST: A parabolic reconstruction of surface tension for the volume-of-fluid method*, J. Comput. Phys., 183 (2002), pp. 400–421.

[48] A. P. S. Selvadurai, *Partial Differential Equations in Mechanics* 2: *The Biharmonic Equation, Poisson's Equation*, Springer, Berlin, Heidelberg, 2000.

[49] N. Sukumar, D. L. Chopp, N. Moës, and T. Belytschko, *Modeling holes and inclusions by level sets in the extended finite-element method*, Comput. Methods Appl. Mech. Engrg., 190 (2001), pp. 6183–6200.

[50] N. Sukumar, Z. Y. Huang, J. H. Prévost, and Z. Suo, *Partition of unity enrichment for bimaterial interface cracks*, Internat. J. Numer. Methods Engrg., 59 (2004), pp. 1075–1102.

[51] F. Wang, Y. Xiao, and J. Xu, *High-Order Extended Finite Element Methods for Solving Interface Problems*, preprint, https://arxiv.org/abs/1604.06171v1, 2016.

[52] T. Warburton and J. S. Hesthaven, *On the constants in hp-finite element trace inverse inequalities*, Comput. Methods Appl. Mech. Engrg., 192 (2003), pp. 2765–2773.

[53] J. Xu, *Estimate of the convergence rate of the finite element solutions to elliptic equation of second order with discontinuous coefficients*, Natural Sci. J. Xiangtan University, 1 (1982), pp. 1–5.

[54] Q. Zhuang and R. Guo, *High Degree Discontinuous Petrov-Galerkin Immersed Finite Element Methods Using Fictitious Elements for Elliptic Interface Problems*, J. Comput. Appl. Math., to appear.

[55] M. Zlámal, *Curved elements in the finite element method*, I, SIAM J. Numer. Anal., 10 (1973), pp. 229–240, https://doi.org/10.1137/0710022.